การพัฒนาเจลอิเล็กโทรไลต์ในแบตเตอรี่ตะกั่ว-กรดแบบมีวาล์วควบคุม
โดยใช้วัสดุเชิงประกอบกราฟีน-พอลิแอนิลีน

นางสาวสุลัดดา ประชันกลาง

วิทยานิพนธ์นี้เป็นส่วนหนึ่งของการศึกษาตามหลักสูตรปริญญาวิทยาศาสตรมหาบัณฑิต
สาขาวิชาปิโตรเคมีและวิทยาศาสตร์พอลิเมอร์
คณะวิทยาศาสตร์ จุฬาลงกรณ์มหาวิทยาลัย
ปีการศึกษา 2557

DEVELOPMENT OF GEL ELECTROLYTE IN VALVE REGULATED LEAD-ACID BATTERY USING GRAPHENE-POLYANILINE COMPOSITE

Miss Suladda Prachanklang

A Thesis Submitted in Partial Fulfillment of the Requirements
for the Degree of Master of Science Program in Petrochemistry and Polymer Science
Faculty of Science
Chulalongkorn University
Academic Year 2014

Thesis Title	DEVELOPMENT OF GEL ELECTROLYTE IN VALVE REGULATED LEAD-ACID BATTERY USING GRAPHENE-POLYANILINE COMPOSITE
By	Miss Suladda Prachanklang
Field of Study	Petrochemistry and Polymer Science
Thesis Advisor	Professor Orawon Chailapakul, Ph.D.

Accepted by the Faculty of Science, Chulalongkorn University in Partial Fulfillment of the Requirements for the Master's Degree

.....Dean of the Faculty of Science

(Professor Supot Hannongbua, Dr.rer.nat.)

THESIS COMMITTEE

.....Chairman

(Assistant Professor Warinthorn Chavasiri, Ph.D.)

.....Thesis Advisor

(Professor Orawon Chailapakul, Ph.D.)

.....Examiner

(Associate Professor Wimonrat Trakarnpruk, Ph.D.)

.....External Examiner

(Assistant Professor Weena Siangproh, Ph.D.)

สุลัดดา ประชันกลาง : การพัฒนาเจลอิเล็กโทรไลต์ในแบตเตอรี่ตะกั่ว-กรดแบบมีวาล์วควบคุมโดยใช้วัสดุเชิงประกอบกราฟีน-พอลิแอนิลีน (DEVELOPMENT OF GEL ELECTROLYTE IN VALVE REGULATED LEAD-ACID BATTERY USING GRAPHENE-POLYANILINE COMPOSITE) อ.ที่ปรึกษาวิทยานิพนธ์หลัก: ศ. ดร.อรวรรณ ชัยลภากุล, 93 หน้า.

ในงานวิจัยนี้เป็นการศึกษาสารเติมแต่งชนิดใหม่ในเจลอิเล็กโทรไลต์ของแบตเตอรี่ตะกั่ว-กรดแบบมีวาล์วควบคุม ได้แก่ กราฟีน วัสดุเชิงประกอบกราฟีน-พอลิแอนิลีน และวัสดุเชิงประกอบกราฟีน-พอลิไวนิลไพโรริโดน-พอลิแอนิลีน เจลอิเล็กโทรไลต์ถูกเตรียมโดยผสมฟูมซิลิกา กรดซัลฟูริกเข้มข้น และสารเติมแต่งด้วยโฮโมจิไนเซอร์ที่มีอัตราการกวนสูง ณ อุณหภูมิห้อง พฤติกรรมทางเคมีไฟฟ้าและประสิทธิภาพของแบตเตอรี่ตะกั่ว-กรดแบบมีวาล์วควบคุมถูกศึกษาด้วยเทคนิคไซคลิกโวลแทมเมทรี อิเล็กโทรเคมิคอลอิมพีแดนซ์สเปคโทรสโคปี ทดสอบความสามารถในการเก็บและคายประจุไฟฟ้า ในการศึกษาลักษณะจำเพาะเชิงสัณฐานวิทยาของขั้วไฟฟ้าใช้เทคนิคสแกนนิงอิเล็กตรอนไมโครสโกปี เทคนิคทรานมิสชันอิเล็กตรอนไมโครสโกปีและเทคนิคอินฟราเรดสเปคโทรสโกปี ผลการทดลองพบว่าเจลอิเล็กโทรไลต์ที่มีวัสดุเชิงประกอบกราฟีน-พอลิแอนิลีน มีความต้านทานการเคลื่อนที่ของประจุต่ำที่สุดเมื่อเปรียบเทียบกับกราฟีน และวัสดุเชิงประกอบกราฟีน-พอลิไวนิลไพโรริโดน-พอลิแอนิลีน หลังจากนั้นมีการศึกษาความเข้มข้นของวัสดุเชิงประกอบกราฟีน-พอลิแอนิลีนที่เติมลงไปในอิเล็กโทรไลต์ระหว่าง 5 และ 60 ส่วนในล้านส่วน พบว่าความเข้มข้นของวัสดุเชิงประกอบกราฟีน-พอลิแอนิลีน ที่ 20 ส่วนในล้านส่วนให้ความต้านทานการเคลื่อนที่ของประจุต่ำที่สุด นอกจากนี้เจลอิเล็กโทรไลต์ที่มีวัสดุเชิงประกอบกราฟีนพอลิแอนิลีนให้ค่าความสามารถในการคายประจุสูงกว่าเจลอิเล็กโทรไลต์ที่ไม่มีสารเติมแต่ง ดังนั้นการเติมแต่งสารเติมแต่งวัสดุเชิงประกอบกราฟีน-พอลิแอนิลีนจึงช่วยเพิ่มประสิทธิภาพของแบตเตอรี่อย่างมีนัยสำคัญ

สาขาวิชา ปิโตรเคมีและวิทยาศาสตร์พอลิเมอร์ ลายมือชื่อนิสิต.....

ปีการศึกษา 2557 ลายมือชื่อ อ.ที่ปรึกษาหลัก.....

5572162723 : MAJOR PETROCHEMISTRY AND POLYMER SCIENCE
KEYWORDS: GELLED ELECTROLYTE / COMPOSITE GRAPHENE-POLYANILINE / VALVE REGULATED LEAD-ACID BATTERY / VRLA BATTERY

SULADDA PRACHANKLANG: DEVELOPMENT OF GEL ELECTROLYTE IN VALVE REGULATED LEAD-ACID BATTERY USING GRAPHENE-POLYANILINE COMPOSITE. ADVISOR: PROF. ORAWON CHAILAPAKUL, Ph.D., 93 pp.

In this work, novel additives in the gelled electrolyte of valve-regulated lead-acid (VRLA) battery were studied, including graphene (GP), graphene-polyaniline (GP-PANI), and graphene-polyvinylpyrroridone-polyaniline (GP-PVP-PANI). Gelled electrolyte was prepared by mixing fumed silica, concentrated sulfuric acid, and additives with high stirring rate of homogenizer at room temperature. The electrochemical behavior and performance of VRLA battery were investigated by cyclic voltammetry (CV), electrochemical impedance spectroscopy (EIS), and galvanostatic charge-discharge method. The morphology of battery plates was characterized by scanning electron microscope (SEM), transmission electron microscopy (TEM), and infrared spectroscopy (IR). The results were found that gelled electrolyte containing GP-PANI provided the lowest charge transfer resistance comparing to the one containing GP and GP-PVP-PANI. After that, various GP-PANI concentrations between 5 and 60 ppm added into the gelled electrolyte were investigated. The lowest charge transfer resistance was obtained at 20 ppm of GP-PANI. Furthermore, gelled electrolyte containing GP-PANI additives provided higher discharge capacity than the conventional gel electrolyte without GP-PANI additive. Therefore, the addition of GP-PANI additive showed the significant improvement of battery performance.

Field of Study : Petrochemistry and Polymer Science Student's Signature.....

Advisor's Signature.....

Academic Year:2014

ACKNOWLEDGEMENTS

Foremost, I would like to express my deepest thanks to my thesis advisor, Professor. Dr. Orawon Chailapakul for her suggestion, advice, guidance, encouragement, and excellent support, which have helped me to solve or overcome problems encountered during different phases of my Master's Degree study at Chulalongkorn University. Thank to my thesis examination committee, Assistant Professor Dr.Warinthorn Chavasiri, Associate Professor Dr.Wimonrat Trakarnpruk and Assistant Professor Dr.Weena Siangproh, who give helpful comment and advice in this thesis. My sincere appreciation is also extended to the committee member, Assistant Professor Dr. Weena Siangproh, for her many suggestions. I would like to thank the N.V. Baterry Ltd, Mr. Krisana Watakeyanon and Ms. Preeyaporn Sangarattanapimanfor their knowledge, time, place and batteries throughout this research. Special thanks also go to all members of Electrochemistry and Optical Spectroscopy Research Unit at Chulalongkorn University for their kindness, friendship and support, especially Mr. Poomrat Rattanarat, Ms. Pattarachaya Preechakasedkit, Ms. Nipapan Ruecha and Mr.Eakkasit Punrat. Also, I gratefully thanks to the financial support from the Thailand Research Fund, Center of Excellence for Petroleum, Petrochemicals, Asian Development Bank and Advanced Materials and CU Graduate School Thesis Grant. Moreover, I would like to thank Chulalongkorn University for partial financial supports and for giving the opportunity to study, laboratory facilities, chemicals and equipments. Lastly, I would like to give my special thanks to my family for showing faith in me, giving me liberty to choose what I desired, and standing behind me with their love and support.

CONTENTS

Page

Page

Page

Page

Page

LIST OF TABLES

LIST OF FIGURES

LIST OF ABBREVIATIONS

a	effective area
ai	activity of the reacting component
A	ampere
ABS	acrylonitrile butadiene stryrene
AC	alternating current
AGM	absorptive glass-mat
Ah	Ampere hour
AGM	absorptive glass-mat
Ah	Ampere hour
C	conductivity
CE	counter electrode
CSCE	colloid silica gelled
CV	cyclic voltammetry
D	distance
DC	direct current
ev	electron volt
E^0	Nernst-potential
F	Faraday constant
FSGE	fumed silica gelled electrolyte
GP	graphene
HEV	hybrid electric vehicles
I	current
IL	ionic liquid
J	Joule
K	degree of Kelven
L	length

mol	mole
mS	mili Siemens
mV	mili volt
M	molar
M_n	number average of molecular weight
M_w	weight average of molecular weight
MF	maintenance-free
PBGE	polysiloxane-based gelled electrolyte
PANI	polyaniline
PVP	polyvinylpyrrolidone
rpm	revolutions per minute
R	resistivity
RE	reference electrode
sp.gr.	specific gravity
S	Siemens
SD	standard deviation
SiO_2	fumed silica
SLA	seal lead-acid
t	time
T	temperature
TEM	transmission electron microscopy
T_g	glass temperature
T_m	melt temperature
U^0	equilibrium voltage
UPS	uninterruptible power supply
V	voltage
VRLA	valve regulate lead-acid
w/v	weight by volume

wt%	weight-weight percentage
W	Watts
WE	working electrode
Wh	Watts-hour
Ω	Ohm
σ	specific conductivity

CHAPTER I

INTRODUCTION

1.1 Introduction

Currently, the energy demand has been rapidly increased while primary energy resources, such as petroleum, natural gas, are limited. Therefore, renewable energy has significantly attracted, especially energy storage as battery used in conjunction with renewable energy sources.

The oldest type of rechargeable batteries and one of the most important in secondary batteries is lead acid batteries or flooded lead acid batteries. These batteries are extensively used in automotive, hybrid electric vehicles (HEV), uninterruptible power supplies (UPS), solar traffic lights, telecommunications, and stationary applications because of their low cost manufacture, easy construction, low self-discharge, and good specific power. However, there are many problems such as acid stratification, leakage of electrolyte, periodic maintenance, and corrosion. To overcome these problems, maintenance-free (MF) valve regulated lead-acid (VRLA) batteries have been developed. There are two technologies for MF-VRLA batteries. First, an absorptive glass mat (AGM) separators is used to immobilize liquid electrolyte. For the second, electrolyte is mixed with gelling agent to form a gelled electrolyte [1]. Hence, the combination between AGM and gel electrolyte are interesting. For the advantage of this combination, it does not require water adding to maintain electrolyte because the water loss is lower than flooded electrolyte. Moreover, the corrosion problem and impact stratification are reduced, in contrast long service life, being able to install any orientation and the cycling performance are increased.

Nowadays, the development of materials as additives with high specific capacitance and great cycle life for batteries is very attractive. Various additives have

been studied such as ionic liquid [2-4], poly (methyl methacrylate), vaniline, polypyrrole, polyacrylamide [5], polyaspartate [6], veratraldehyde [7], graphite [8], and so on.

Graphene (GP), a two dimensional sheet of sp^2 carbon atom, has become an outstanding nanomaterial in electrochemistry [9-12] due to good chemical stability, high electrical and thermal conductivity, excellent mechanical properties, and large surface area [13]. However, GP shows high tendency to agglomerate and restack to form graphite through p–p stacking and Vander Waals interactions which make the used of GP is limited in some applications [14, 15]. Therefore, the composites between GP and conducting polymers have more attractive than the pure form of GP because the agglomeration is reduced [16].

Conducting polymers have been extensively studied and widely applied in various electrochemical device and energy storage. Among various the conductive polymers, polyaniline (PANI) is considered to be one of the most useful conducting polymers because of its environmental stability, ease of synthesis, and simple doping/dedoping chemistry [17-19].

In this work, graphene-polyaniline (GP-PANI) additive was developed for gel absorptive glass mat valve-regulated lead-acid (AGM-VRLA) batteries to improve the electrochemical and battery performance. Moreover, the developed gelled electrolyte filled in (AGM-VRLA) batteries was tested. It was found that the water loss is minimized while the cycling ability is improved.

1.2 Objectives of the Research

(i) To develop gelled electrolyte in valve-regulated lead-acid (VRLA) batteries using graphene-polyaniline additive.

(ii) To study electrochemical and physical properties of gelled electrolyte with graphene-polyaniline additive.

(iii) To test the performance of gel batteries by measuring the discharge capacity.

1.3 Scope of the Research

To achieve the objectives of the research, the following scopes are set.

(i) Literature reviews of VRLA batteries, gelled electrolytes, graphene, and polyaniline.

(ii) Investigating gel time and gel hardness of gelled electrolyte with graphene-polyaniline additive.

(iii) Studying electrochemical behavior of gelled electrolyte with graphene-polyaniline additive by cyclic voltammetry and electrochemical impedance spectroscopy.

(iv) Investigating the discharge capacity of developed gel batteries, and morphology of the gelled electrolyte.

(v) Finally, all the results are discussed.

CHAPTER II

THEORY AND LITERATURE REVIEW

Battery is a device which can store chemical energy and convert it to electrical energy. A chemical process occurred, that generates energy, can be drawn from the battery in form of an electric current at a certain voltage. In battery system, this process can be reversed, that the battery recharged by an intake of electrical energy. The chemical composite in the battery can be turned into the original structure that contains higher energy.

Battery can be divided into two major classes:

(1) Primary battery that is designed to convert its chemical energy into electrical energy only once, for example, carbon-zinc (Leclanche or dry cell), alkaline-manganese, mercury zinc, silver-zinc, and lithium cells (e.g., lithium-manganese dioxide, lithium-sulfur dioxide, and lithiumthionyl chloride).

(2) Secondary battery a reversible energy converter that is designed for repeating discharges and charges. It is genuine electrochemical storage systems, for instance, lead-lead dioxide (lead-acid), nickel-cadmium, nickel-iron, nickel-hydrogen, nickel-metal hydride, silver-zinc, silver-cadmium, and lithium-ion.

2.1 Lead-acid Battery

Lead acid battery was invented by French physicist Gaston Planté in 1860. At the first, it was used for keeping the light on of railroad cars stopped at train stations and for providing a standby power for utilities and commercial use for over century. The events in technical developments of lead acid battery are shown in Table 2.1.

From first developments of Planté, various experiments were done on accelerating a formation process and coating lead foil with lead oxides on a lead plate pretreated by the Planté method. Concentration then turned to other methods for retaining active material, and two main technological paths are evolved.

(1) Coating a lead oxide paste on cast or expanded grids, rather than foil, in which structural strength and retention properties of the active material are developed by a ‘‘cementation’’ process (interlocked crystalline lattice) through the grid and active mass. This is generally referred to flat-plate design.

(2) The tubular electrode design, in which a central conducting wire or rod is enclosed by active material. And the assembly is covered in an electrolyte porous insulated tube, which is either square, round, or oval.

Simultaneous advances in developing and retaining active material were worked in strengthening the grid by casting it from lead alloys such as lead-antimony (e.g., Sellon, 1881) or lead-calcium (e.g., Haring and Thomas, 1935). The technical knowledge for an economical manufacture of reliable lead-acid batteries was in place by the end of the 19th century, and the subsequent growth in the industry was rapid. The technology of battery was developed in the mid-1970s when researchers developed a maintenance-free lead-acid battery that was able to operate in any position. There have been strong demands for production of low-maintenance or maintenance-free batteries. Until ten years ago, however, these batteries secured only niche-products. In the 1980s, when the technology was scaled-up to 3000 Ah, a high state of attention was shown in such designs and a worldwide development for valve-regulated batteries commenced [20].

Table 2.1 Events in technical development of lead-acid battery

Precursor systems		
1836	Daniell	Two-fluid cell; copper/copper sulfate/sulfuric acid /zinc
1840	Grove	Two-fluid cell; carbon/fuming nitric acid / sulfuric acid/ zinc
1854	Sindesten	Polarized lead electrodes with external source
Lead acid battery developments		
1860	Plantè	First practical lead-acid battery, corroded lead foils to form active material

Lead acid battery developments		
1881	Sellon	Lead-antimony alloy grid
1881	Volckmar	Perforated lead plates to provide pockets for support of oxide
1882	Brush	Mechanically bonded lead oxide to lead plates
1882	Gladstone and Tribs	Double sulfate theory of reaction in lead-acid battery: $PbO_2 + Pb + 2H_2SO_4 \leftrightarrow 2PbSO_4 + 2H_2O$
1883	Tudor	Pasted mixture of lead oxides on grid pretreated by Planté method
1886	Lucas	Formed lead plates in solutions of chlorates and perchlorates
1890	Phillipart	Early tubular construction-individual rings
1890	Woodward	Early tubular construction
1910	Smith	Slotted rubber tube, Exide tubular construction
1920 to Present		Materials and equipment research, especially expanders, oxides,and fabrication techniques
1935	Haring and Thomas	Lead-calcium alloy grid
1935	Hamer and Harned	Experimental proof of double sulfate theory of reaction
1956–1960	Bode and Voss Ruetschi and Cahan Burbank Feitknecht	Clarification of properties of two crystalline forms of PbO_2 (alpha and beta)

Lead acid battery developments		
1970s	McClelland and Devit	Commercial spiral-wound sealed lead acid battery. Expanded metal grid technology; composite plastic/ metal grids; sealed and maintenance-free lead-acid batteries; glass fiber and improved separators; through-the-partition intercell connectors; heat-sealed plastic case-to-cover assemblies; high-energy density batteries (above 40 Wh/ kg); conical grid (round) cell for long-life float service in telecommunications facilities
1980s		Sealed valve-regulated batteries; quasi-bipolar engine starter batteries; improved low-temp. performance; world's largest battery installed (Chino, Calif.); 40-MWh lead-acid load leveling
1990s		Electric-vehicle interest reemerges; bipolar battery designs for High power use in uninterruptible power supplies, power tool market and electronic back-up. Thin foil cells, small cells for consumer and current road applications.
2000s		Planned introduction of 36 Volt SLI battery system for automobiles

2.1.1 Types of Lead-acid Battery

Lead-acid battery can be divided into 2 types.

(1) A conventional lead-acid battery consists of negative and positive plates, which are made from lead and lead dioxide, respectively, immersed in sulfuric acid electrolyte. This battery is generally called ‘‘flooded lead-acid battery’’. Due to its simple design, it allows the hydrogen and oxygen gases generated during the charge cycle to vent to the atmosphere. So distilled water must be added to maintain a volume and a concentration of the electrolyte. Accordingly, it requires the regular maintenance.

(2) Valve-regulated lead-acid (VRLA) battery, also known as sealed lead-acid battery, has been developed to reduce the water loss of battery and to eliminate the need of any maintenances. This battery consists of pressure-release valves for allowing the gases releasing when the internal pressure exceeds a certain level. It is designed to use an immobilized electrolyte so that oxygen generated during the charge cycle is captured and recombined in the battery leading to less or no water loss. Hence, this battery is also called ‘‘oxygen recombination cycle’’.

2.1.2 Advantages and Limitations of Lead-acid battery

There are a lot of advantages and good reason that lead-acid battery is still widely used nowadays. Lead-acid is dependable and inexpensive on a cost-per-watt base. This value is rather low compared to other systems. There is a few of other batteries that can deliver bulk power as cheaply as lead acid, It makes the battery cost-effective for automobiles, golf cars, forklifts, marine, and uninterruptible power supplies (UPS). A limitation of lead-acid battery is heavier compared to other type of batteries. Moreover, it is less durable than nickel- and lithium-based systems in deep-cycled. However, lead-acid battery is still the most commonly used battery due to its other factors; (i) the cost of the battery is only 65-70% of the cost of

nickel/cadmium battery, (ii) the charge characteristic is simple because the current is controlled by the state-of-charge, (iii) environmental problems are less than from nickel/cadmium battery and lead can recycled fully.

2.2 Valve Regulated Lead-acid (VRLA) Battery

A newer designed lead-acid battery is called ‘‘Valve-Regulated Lead-Acid Battery’’ or VRLA. It is different from the conventional flooded lead-acid battery by containing only a limited amount of electrolyte (starved electrolyte) absorbed in the separator or immobilized in the gel. In general designs, the cell capacity is limited by the amount of positive active material. The starved electrolyte and excess of negative active material simplify the recombination of oxygen produced during overcharge or ‘‘float’’ charge with the negative active material. The resalable valves are normally closed to prevent the entrance of oxygen from the outside. A vent pressure design is depended on the manufacturer and predominantly by the case shape and material. There are two usual shapes in VRLA designs. One is spirally-wound electrodes (jelly-roll construction) in a cylindrical container, and the second is flat plates in a prismatic container. The cylindrical containers can maintain higher internal pressures and it can be designed to release pressure better than the prismatic container. In some designs, an outer metal container is used to prevent deformation of the plastic case by high temperature and the internal cell pressure. The range of venting pressures includes a high of 25 to 40 psi for a metal-sheathed, and spirally wound cell to 1 to 2 psi for a large prismatic battery.

Recently, two product technology concepts for immobilizing the electrolyte within the cell of VRLA battery are in commercial production including;

First is an absorptive glass-mat (AGM) separator of which liquid electrolyte is adsorbed in the porous separator. The passage for oxygen can occur under saturation of the electrolyte in the separator.

Second is a gelled electrolyte in which fumed silica or sub-micron diameter silicon dioxide is added to the electrolyte and can cause it to harden in form of gel. This gel has a good thixotropic property so it can be poured into the cell. Moreover, the immobilization of the electrolyte allows battery to operate in different orientations without spillage.

VRLA battery designs became more popular for over 75% of telecommunication and UPS applications in 1999. The development of advance charging techniques can increase the use of VRLA batteries in cycling applications such as forklift service. New market opportunities in power tools, portable electronics and hybrid electric vehicles have stimulated the development of new designs of lead-acid batteries.

However, the VRLA designs have not the capability of handling certain types of abuse as well as conventional flooded batteries. The electrolyte, which provides the major internal heat sink in cells, is more limited in the VRLA cell. Consequently, VRLA designs are more inclined to thermal runaway under an abusive condition that poses little hazard in flooded cells. In fact, VRLA batteries are subjected to be operated at elevated temperatures. Therefore, the high temperature (over 40°C) effect, advantages and disadvantages have been discussed.

To insure that battery has a long life under high temperature operations or overheating due to oxygen recombination, the precaution must be taken. A comparison between gel designs and absorbed electrolyte designs in fork lift truck applications was presented for one particular set of applications. However, new materials and designs are developed, and the comparisons should be ongoing. Much activity has been reported in the area of special fibers, blends, and surface treatments for absorbing mat separators. The major advantages and disadvantages of VRLA batteries are listed in Table 2.2

Table 2.2 Major Advantages and Disadvantages of VRLA Batteries

Advantages	Disadvantages
Maintenance-free	Should not be stored in discharged condition
Moderate life on float service	Relatively low energy density
High-rate capability	Lower cycle life than sealed nickel-cadmium battery
High charge efficiency	More sensitive to higher temperature environment than conventional lead-acid batteries
No ‘‘memory’’ effect (compared to nickel-cadmium battery)	Thermal runaway can occur with incorrect charging or improper thermal management
Relatively low cost	

2.2.1 Construction of VRLA Battery

The active mass is fixed in a lead-based grid that is chemically resistant to H_2SO_4 solution.

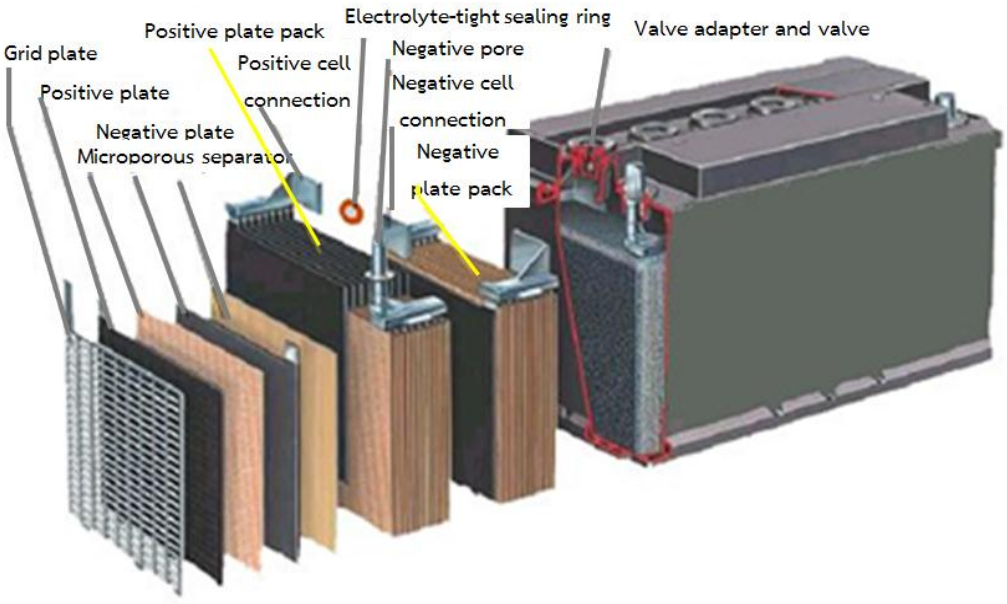

Figure 2.1 Cut-away cell of VRLA battery showing details of construction [21]

2.2.1.1 Electrode (Plate)

Plate construction is the key to produce a good battery. It employs the latest technology and equipment to cast grids from a lead-calcium alloy free of antimony. The small amount of calcium and tin in the grid alloy imparts strength to the plate and guarantees durability even in extensive cycle service. Positive and negative plates contain materials capable of reacting with electrolyte to produce or accept current.

Positive Plates (PbO)

Positive plates are plate electrodes that a grid frame of lead-tin-calcium alloy holds porous lead dioxide as the active material.

Negative Plates (Pb)

Positive plates are plate electrodes that a grid frame of lead-tin-calcium alloy holds porous lead dioxide as the active material.

2.2.1.2 Grid Support

Grid or plate support has to provide mechanical support for the active material and electronic conductivity for the collected current. Early grid materials for VRLA batteries consisted of pure lead or lead cadmium alloys for both the positive and negative plates. The selection of grid alloys must not only consider fabrication requirements, mechanical strength, but also corrosion resistance and creep strength, and must pay attention to the electrochemical problems. Many additive were added to grid allot such as tin (Sn), antimony (Sb), cadmium (Cd), aluminium (Al), etc.

2.2.1.3 Electrolyte (H_2SO_4)

The electrolyte used in lead-acid batteries is diluted sulfuric acid (H_2SO_4). Diluted sulfuric acid is used as the medium for conducting ions in the

electrochemical reaction in the battery. In contrary to other electro-chemical systems, electrolyte of lead-acid accumulators takes part at the chemical reaction and will be more diluted during discharge because of water formation. This means, the electrolyte density is significantly lower in a discharged lead-acid accumulator than in a charged one. This characteristic clearly distinguishes lead-acid accumulators from other electro-chemical energy storage, and the problem can occur at temperatures below -5°C because the electrolyte might freeze. Thus, the active mass and the containers could be damaged due to an increase of the volume.

2.2.1.4 Separators

Separators can retain electrolyte and prevent shorting between positive and negative plates. They adopt a non-woven fabric of fine glass fibers which is chemically stable in the diluted sulfuric acid electrolyte. Being highly porous, separators maintain electrolyte for the reaction of active materials in the plates. The separator has been used such as polyvinylchloride (PVC), absorbent glass mat (AGM), and polyethylene (PE) for VRLA battery.

2.2.1.5 One Way Valve and Relief Valve

One Way Valve

The valve contains a one-way valve made of material, for example, neoprene. When gas is generated in the battery under extreme overcharge condition because of erroneous charging, charger malfunctions or other abnormalities, the vent valve opens to release excessive pressure in the battery and maintain the gas pressure within specific range (7.1 to 43.6 kPa). During ordinary use of the battery, the vent valve is closed to shut out outside air and prevent oxygen in the air from reacting with the active material in the negative electrodes.

Relief Valve

In case of excessive gas pressure build-up inside the battery (usually caused by abnormal charging), the relief valve will open and relieve the pressure. The one-way valve not only ensures that no air gets into the battery where the oxygen would react with the plates causing internal discharge, but also represents an important safety device in the event of excessive overcharge. Vent release pressure is between 2-6 psi, and the seal ring material is neoprene rubber.

2.2.1.6 Positive and Negative Electrode Terminals

Positive and negative electrode terminals may be fast on tab type, bolt fastening type, threaded post type, or lead wire type, depending on the type of the battery. Sealing of the terminal is achieved by a structure which secures long adhesive-embedded paths and by the adoption of strong epoxy adhesives.

2.2.1.7 Battery Case Materials

Materials of the body and cover of the battery case are ABS, a high-impact proof plastic resin, styrene, or a polypropylene-polyethylene copolymer with resistance to chemicals and flammability.

2.2.2 General Characteristics of VRLA Battery

2.2.2.1 Chemistry

The lead-acid battery uses lead dioxide as the active material of the positive electrode and metallic lead, in a high-surface-area porous structure, as the negative active material. Regularly, a charged positive electrode consists of both α-PbO_2 (orthorhombic) and β-PbO_2 (tetragonal). The equilibrium potential of the α-PbO_2 is more positive than that of the β-PbO_2 by 0.01 V. The α form also has a larger, more compact crystal morphology which is less active electrochemically and slightly lower in capacity per unit weight. However, it promotes longer cycle life.

Neither of the two forms is fully stoichiometric. Their composition can be represented by PbO_X which x is varied between 1.85 and 2.05. The introduction of antimony, especially at low concentrations, for the preparation or cycling of these species leads to a considerable increase in their performance. The preparation of the active material precursor contains a series of mixing and curing operations using leady lead oxide (PbO + Pb), sulfuric acid, and water. The ratios of the reactants and curing conditions (temperature, humidity, and time) can affect the development of crystallinity and pore structure. The cured plate includes lead sulfate, lead oxide, and some residual lead (<5%). The positive active material, which is formed electrochemically from the cured plate, is a major factor influencing the performance and life time of the lead-acid battery. For the negative, electrode controls cold-temperature performance (such as engine starting). The electrolyte is a sulfuric acid solution, which is typically about 1.28 specific gravity or 37% acid by weight in a fully charged condition.

2.2.3 Chemical Reaction

The following chemical reactions clearly describe the exact transformation which occurs both in the positive and negative plates, because of electrochemical processes. As the cell discharges, both electrodes are converted to lead sulfate. The process reverses on charge. The electrochemical reaction processes of the valve regulated lead-acid batteries are described below; [20]

Negative electrode $Pb \underset{\text{Charge}}{\overset{\text{Discharge}}{\rightleftharpoons}} Pb^{2+} + 2e^-$

$Pb^{2+} + SO_4^{2-} \underset{\text{Charge}}{\overset{\text{Discharge}}{\rightleftharpoons}} PbSO_4$

Positive electrode $PbO_2+4H^{+}+2e^{-} \underset{\text{Charge}}{\overset{\text{Discharge}}{\rightleftharpoons}} Pb^{2+}+2H_2O$

$Pb^{2+}+SO_4 \underset{\text{Charge}}{\overset{\text{Discharge}}{\rightleftharpoons}} PbSO_4$

The basic electrochemical reaction equation in a lead-acid battery can be written as follows:

Overall Reaction $Pb + PbO_2 + 2H_2SO_4 \underset{\text{Charge}}{\overset{\text{Discharge}}{\rightleftharpoons}} 2PbSO_4+2H_2O$

2.2.3.1 Discharging process

Discharge is the operation of drawing out electric energy from the battery to operate external equipment. During the discharge portion of the reaction, PbO_2 (lead dioxide; positive plate) and lead (negative plate) react with sulfuric acid to create $PbSO_4$ (lead sulfate), water, and energy. These processes are reversed during the charging phase.

2.2.3.2 Charging process

Charge is the operation of supplying the rechargeable battery with direct current from an external power source to change the active material in the negative plates, and hence to store in the battery electric energy in the form of chemical energy. During the charging phase, the $PbSO_4$ of the positive plate oxidizes and re- forms as PbO_2, while the $PbSO_4$ re-forms as Pb (spongy lead) in the negative plate.

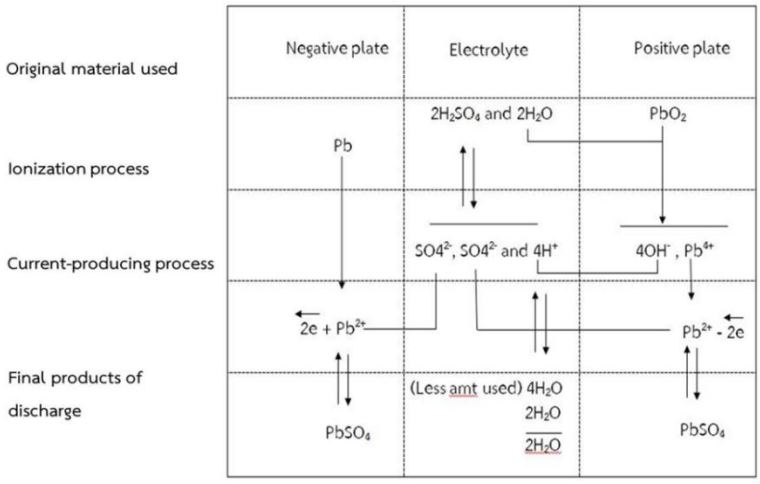

(a)

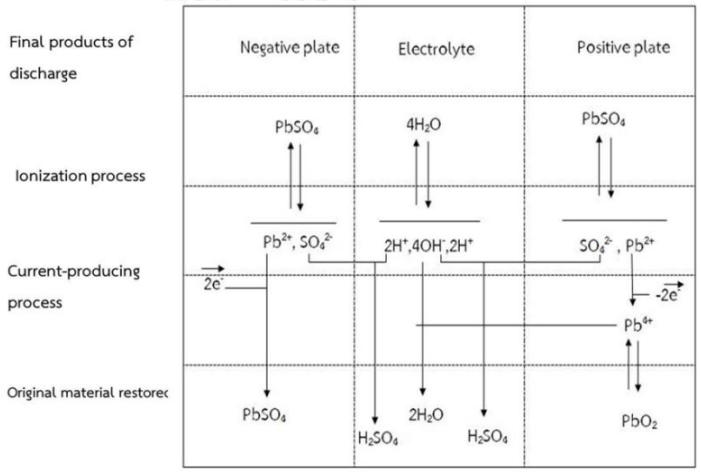

(b)

Figure 2.2 Discharge and charge reactions of lead-acid cell. (a) Discharge reactions (b) Charge reactions [22]

2.2.3.3 Performance of VRLA Battery

The general performance characteristics of lead acid battery, during charge and discharge are shown in Figure 2.3. As the cell is discharged, the voltage decreases because of depletion of material, internal resistance losses, and polarization. If the discharge current is constant, the voltage under load decreases

smoothly to the cutoff voltage, and the specific gravity decreases in proportion to the ampere-hours discharge.

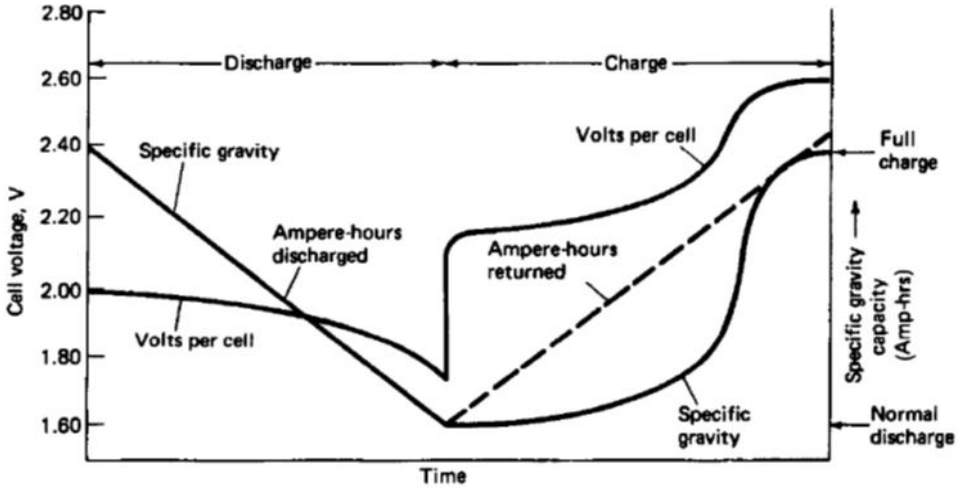

Figure 2.3 Typical voltage and specific gravity characteristics of lead-acid cell at constant discharge and charge [20]

2.2.3.4 Equilibrium Voltage

The dependence of the equilibrium voltage on concentration is given by the Nernst equation. The right hand side of the equation at temperature of 297 K, and the conversion (ln= 2.03.log) can be express for a lead acid battery as:

$$U^{\circ} = 1.932 - \frac{RT}{2F} \cdot In \frac{(a_{H_2O})^2}{(a_{H^+})^2 \cdot \left(a_{HSO_4^-}\right)^2} = 1.932 + 0.0592 \cdot \log \frac{a_{H^-} . a_{HSO_4^-}}{a_{H_2O}} \quad (2.1)$$

Where; U° is the equilibrium voltage of cell (V)

R is the molar gas constant for an ideal gas (8.1314 $J.K^{-1}.mol^{-1}$)

T is the temperature (K)

F is the Faraday constant (96,485 coulumbs/equivalent)

a_i is activity of the reacting component ($mol.cm^{-3}$)

And the equilibrium voltage applies when the activities of the soluble components of the reaction, namely H^+, HSO_4^-, and H_2O amount to 1 mol/dm^3, respectively.

According to this equation the equilibrium voltage depends only on the acid concentration and independent of lead, lead dioxide and lead sulfate which present in the battery.

Results of equation 2.1 are plotted in Figure 2.3 and also compiled in the column "Cell voltage" in the table 2.3 together with the single electrode potentials.

In battery practice, the approximation:

Equation cell voltage = acid density (in g/cm^3 or kg/cm^3) + 0.84 (2.2)

Equation 2.2 is used instead of equation 2.1. Figure 2.4 shows that the calculated curve and the approximate coincide quite well.

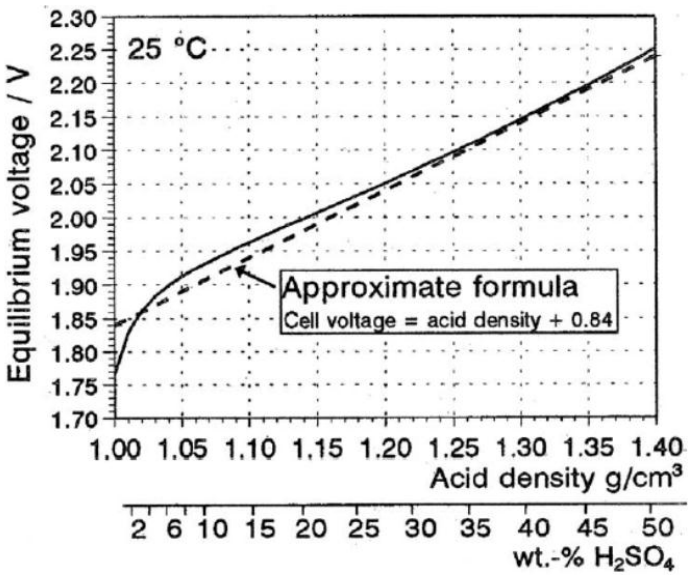

Figure 2.4 Equilibrium cell voltage of the lead-acid battery referred to, acid density, and acid concentration in wt% H_2SO_4. The dash line represents the approximation of equation 2.2

According to equation 2.1, the equilibrium potential depends on the acid concentration. On the other hand, H_2SO_4 participates in the electrode reaction, the electrolyte becomes more dilute during discharge and is re-concentrated during the charge. The participation of H_2SO_4 in the cell reaction has considerable consequences. This could be explained that the cell voltage does not remain constant even at low discharge rate, and the conductivity of acid varies when the battery is charge or discharged. If the discharge occurs cold climates, the acid may be freeze. On the other side, in the flooded cell, acid dilution may be used as tool to determine the state of charge. [23]

Table 2.3 Acid-concentration parameter: acid density (kg/L), H_2SO_4 content and H_2SO_4 concentration in mol/L, and molality. Cell voltage and electrode potentials referred to the standard hydrogen electrode.

Acid-concentration				Cell Voltage U° Volts	Electrode potentials	
Dens.kg/L	H_2SO_4 wt.%	Molarity mol/L	Molality mol/kg H_2O		V ref. to std. Positive	H_2 electrode Negative
1.02	3.48	0.362	0.367	1.860	1.595	-0.265
1.03	5.00	0.525	0.537	1.833	1.607	-0.276
1.04	6.49	0.688	0.708	1.899	1.616	-0.283
1.05	7.77	0.832	0.859	1.913	1.623	-0.290
1.06	9.42	1.018	1.060	1.924	1.630	-0.294
1.07	10.86	1.184	1.242	1.935	1.634	-0.301
1.08	12.28	1.352	1.428	1.945	1.641	-0.304
1.09	13.69	1.521	1.617	1.955	1.645	-0.310
1.10	15.08	1.691	1.811	1.964	1.650	-0.314
1.11	16.45	1.861	2.007	1.973	1.654	-0.319
1.12	17.80	2.032	2.207	1.982	1.659	-0.323
1.13	19.13	2.204	2.412	1.991	1.663	-0.328
1.14	20.46	2.378	2.623	2.000	1.668	-0.332
1.15	21.78	2.553	2.838	2.008	1.673	-0.335

Acid-concentration				Cell Voltage U° Volts	Electrode potentials	
Dens.kg/L	H_2SO_4 wt.%	Molarity mol/L	Molality mol/kg H_2O		V ref. to std. Positive	H_2 electrode Negative
1.16	23.08	2.729	3.059	2.017	1.667	-0.340
1.17	24.36	2.906	3.285	2.026	1.682	-0.344
1.18	25.63	3.084	3.514	2.034	1.687	-0.347
1.19	26.89	3.262	3.749	2.043	1.691	-0.352
1.20	28.14	3.443	3.992	2.052	1.696	-0.356
1.21	29.38	3.625	4.242	2.061	1.700	-0.361
1.22	30.61	3.807	4.498	2.070	1.705	-0.365
1.23	31.83	3.992	4.760	2.079	1.710	-0.369
1.24	33.05	4.178	5.033	2.088	1.715	-0.373
1.25	34.25	4.365	5.311	2.097	1.720	-0.376
1.26	35.44	4.553	5.597	2.107	1.725	-0.381
1.27	36.62	4.742	5.892	2.116	1.730	-0.386
1.28	37.79	4.932	6.194	2.126	1.735	-0.391
1.29	38.95	5.123	6.507	2.136	1.740	-0.396
1.30	40.10	5.315	6.826	2.145	1.745	-0.400
1.31	41.24	5.508	7.155	2.156	1.751	-0.405
1.32	42.37	5.702	7.496	2.166	1.757	-0.409
1.33	43.49	5.897	7.846	2.176	1.762	-0.414
1.34	44.59	6.092	8.206	2.187	1.768	-0.419
1.35	45.68	6.287	8.573	2.197	1.773	-0.424
1.36	46.74	6.482	8.949	2.208	1.778	-0.430
1.37	47.80	6.677	9.336	2.219	1.783	-0.436
1.38	48.85	6.873	9.738	2.230	1.788	-0.442
1.39	49.89	7.070	10.149	2.241	1.794	-0.447
1.40	50.91	7.267	10.573	2.252	1.800	-0.452

2.2.4 Failure Mode of VRLA Battery

2.2.4.1 Overcharge

In the final stage of charging, an oxygen-generating reaction occurs at the positive plates. The oxygen transfers inside the battery and the oxygen is then absorbed into the surface of the negative plates and consumed. These electrochemical reaction processes are expressed as follows;

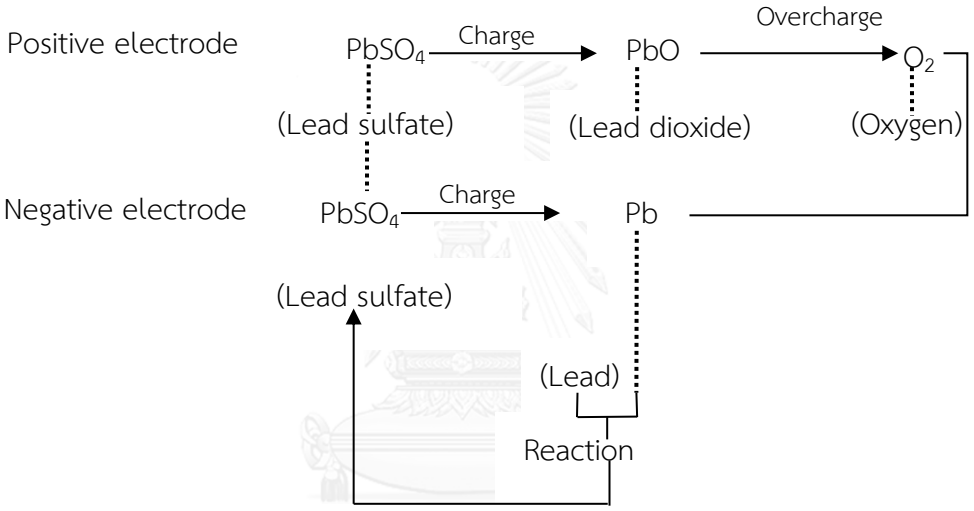

Gas recombination reaction cycle

2.2.4.2 Gassing and Recombination

Gassing of Vented Batteries

A highlight of vented lead-acid batteries is water loss. For electrolysis, oxygen (O_2) is formed at the positive electrode, and hydrogen (H_2) occurs on the negative electrode in a stoichiometric relation of 1:2. Both, oxygen and hydrogen, escape as gas bubbles through the degassing vents because of the low solubility of both gases in the electrolyte.

The equations of the electrode reactions:

Positive Electrode:

$PbO_2 + H_2SO_4 + 2H^+ + 2e^- \rightarrow PbSO_4 + 2H_2O$ (2.3)

$H_2O \rightarrow ½O_2 + 2H^+ + 2e^-$ (2.4)

Negative Electrode:

$Pb + H_2SO_4 \rightarrow PbSO_4 + 2H^+ + 2e$ (2.5)

$2H^+ + 2e^- \rightarrow H_2$ (2.6)

This means, in total, water is being decomposed by the reaction

$2H_2O \rightarrow O_2 + 2H_2$ (2.7)

This water loss is compensated by refilling water in vented batteries. The water loss due to water decomposition depends on the charging mode, the design of cells, the used grid alloy, and the purity of materials, especially these of pure lead and electrolyte. To use alloys at low antimony content (< 3%), the topping-up intervals of vented stationary batteries are currently in the range of 3 to 5 years, depending on the electrolyte reserve between minimum and maximum marking.

Recombination of Valve Regulated Batteries

A highlight of valve regulated lead-acid (VRLA) batteries is the recombination of oxygen during charging. During charging the continuous running circulation starts at the positive electrode:

$H_2O \rightarrow ½ O_2 + 2H^+ + 2e^-$ (2.8)

Water (H_2O) is decomposed, and gaseous oxygen (O_2) is formed. The hydrogen ions (H^+) remain solved in the electrolyte and will not be released as gas. The electrons ($2e^-$) flow through the exterior electrical circuit to the negative electrode. In opposite to a vented system, the oxygen does not escape from a cell in a valve regulated system. The cells are closed by a valve. The oxygen diffuses to the negative plate, where it is converted from lead to lead oxide (PbO):

$Pb + ½ O_2 \rightarrow PbO$ (2.9)

The oxygen transfer in VRLA-batteries takes place via a solid porous medium by cracks the gel or free pores of the fleece material. In vented lead-acid batteries with “free” (liquid) electrolyte, which means not starved electrolyte, it is almost impossible that the oxygen migrates to the negative electrode due to the low solubility. It rises directly after leaving the positive electrode as gas bubbles and escapes via the cell vents. Figure 2.5 displays the comparison between vented and VRLA-batteries.

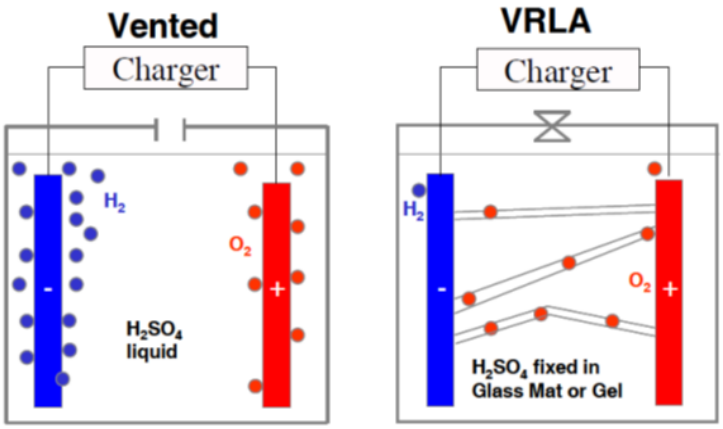

Figure 2.5 Gassing and recombination of vented and VRLA-batteries [24]

The produced lead oxide is not stable in sulfuric acid (H_2SO_4) and will be converted to lead sulfate. And, water is produced as a by-product:

$$PbO + H_2SO_4 \rightarrow PbSO_4 + H_2O \qquad (2.10)$$

This means that the negative electrode is partially discharged during charging in VRLA-batteries. This partial discharge during charging of the negative electrode is essential and deliberated to suppress the hydrogen formation.

The partial discharge of the negative electrode is executed by oversizing of the negative electrode. By the float current, the lead sulfate is converted back to metallic lead:

$$PbSO_4 + 2\,H^+ + 2e^- \rightarrow Pb + H_2SO_4 \quad (2.11)$$

From energetic point of view, the reactions of the equation are preferred, comparing to the formation of hydrogen at the negative electrode. Therefore, the formation of the hydrogen is suppressed by recombination. The process of recombination is exothermic, so that VRLA-batteries hold a confident risk of Thermal Runaway. The effectiveness of recombination of VRLA-batteries is regularly 98% for Gel-batteries and 99% for AGM-batteries. The remaining 1 – 2 % oxygen can lead to the formation of hydrogen at the negative plate. If a defined opening pressure is reached, the valve opens for a short time, and the collected gas can escape. To use antimony-free alloys for VRLA-batteries, the water loss can be decreased about 75% in comparison to vented batteries. For the recombination, the water loss can be decreased to 98 till 99%, so less than 2% of water loss can be achieved by a valve regulated system. This is the reason why water refilling is not essential during the complete service life of a VRLA-battery.

2.2.4.3 Electrolyte Stratification

The electrolyte in a lead acid battery contains water and sulfuric acid which ideally would be thoroughly mixed. However, sulfuric acid is denser than water, a situation can occur where the acid concentration at the bottom of the battery is higher than at the top. This situation will reduce the performance of the battery. Stratification can develop if a battery is not being fully charged (when a battery is fully charged some gassing will cause a mixing of the electrolyte) and if the battery is static (no movement to help mixing). Stratification itself will not have a permanent effect on the performance of battery. A single full charge should sufficiently mix the electrolyte, although a battery left in a stratified state may result in sulphation when the acid concentration is high.

Acid stratification is often the reason for the failure of batteries with low values of water decomposition. Electrolyte stratification is connected with the changes of specific weight of the electrolyte associated with the concentration changes during charge and discharge. In the flooded lead-acid batteries, an acid stratification may cause extreme problems. The immobilization of the electrolyte in VRLA batteries can reduce stratification effects to large extent, or practically eliminates them in gelled electrolyte.

During charge, sulfuric acid is released from the active material in the plates, and the concentration of the acid increases between the plates. The highest acid concentration is achieved between plates which initiate convection of this acid to the parts beside and underneath the plates. At the end of charging process, the battery is filled with a slightly increase of acid concentration to the upper edge of the plates. The acid above the plates remains diluted and there is no driving force for convection due to the low weight of acid.

In the usual stationary application, acid stratification causes no problems, because the batteries are only discharged at times. There is enough time left for the diffusion to equalize the acid concentration. In addition, acid stratification may become dangerous because the concentration differences between the top and bottom part of the cell are growing from cycle to cycle, especially in tall cell. The increasing of acid concentration at the bottom may harm the negative plate, which is prone to sulphation when running in too high an acid concentration.

As a remedy stratification, overcharging by 10 to 20% during each cycle is mostly applied for traction battery. The gas evolution forms bubbles that mix the electrolyte. An immobilization of the electrolyte, as required for VRLA batteries, eliminates stratification effects almost completely.

2.2.4.4 Electrolyte Loss

High temperatures, high charging rates, and over charging can cause a loss of electrolyte in non-sealed batteries. In sealed batteries, the same factors will cause an increase in temperature and pressure which can ultimately result in the release of gas (and possibly electrolyte) from valves. Any loss of electrolyte resulting in part of the plates being above the electrolyte surface will result in reduction of battery performance.

2.2.4.5 Sulphation

When lead acid battery discharges, lead sulphate crystals are deposited on the plates as part of the normal chemical reaction that results in the flow of electrons (at the same time, the sulfuric acid electrolyte is being converted to water). During charging, the chemical reaction is reversed, and the lead sulphate crystals are converted back to lead on the negative electrode and lead oxide on the positive electrode. If the battery is left for sometime not fully charged, or is in use but not reaching a fully charged state, the lead sulphate crystals will harden and will not convert back to lead or lead oxide during charging. This effect will happen more rapidly at higher temperatures. Once this happens, the capacity of the battery will be reduced.

2.2.4.6 Separator Failure

If two battery plates come into contact, cell will suffer a short, and a 12 volt battery will effectively become a 10 volt battery. Plate contact can occur if the separator material breaks down or plates become distorted because of excessive heat. Overcharging can cause plate distortion.

2.2.4.7 Thermal Runaway

A critical condition a rises during constant charging when the rate of heat production in a battery exceeds its heat dissipation capability causing a continuous temperature increase which can lead to the destruction of the battery.

Vented lead batteries are not affected from thermal runaways practically due to the high electrolyte volume and the excellent heat transfer. Similar is valid for gel-batteries in comparison with AGM-batteries because of the fact, that gel-batteries have nearly the same volume of electrolyte as vented batteries, but AGM-batteries have significant less electrolyte comparing to both other technologies. Compared to vented and gel-batteries, AGM-batteries produce much more heat because of the very high recombination rates due to the large free volume in the separator (fleece). Furthermore, the heat can be derivated not so easily because of the smaller electrolyte volume as well as the lower wetting of the internal walls with electrolyte. Therefore, AGM-batteries, operated under harsh conditions such as high environmental temperatures, missing or insufficient air conditioning, missing or wrong temperature compensation of the charging voltage, tend more easy to thermal runaways. Concerning installation of VRLA-batteries, especially the distances between cells respectively blocks of minimum 5 mm (recommended 10 mm) need to be mentioned. The operating instructions content furthermore the hint, that the batteries have to be installed in a manner, that between the single cells respectively blocks no environment-induced temperature differences of more than 3 K can occur.

2.2.4.8 Self-discharge

The equilibria of the electrode reactions are normally in the discharge direction because the discharged state is thermodynamically stable. The rate of self-discharge loss of capacity (charge) when no external load is applied of

the lead-acid cell is fairly quick, but it can be reduced significantly by incorporating certain design features. The rate of self-discharge depends on some factors. Lead and lead dioxide are thermodynamically unstable in sulfuric acid solutions, and on open circuit. Hence, they can react with the electrolyte. Oxygen is evolved at the positive electrode and hydrogen at the negative, at a rate dependent on temperature and acid concentration (the gassing rate increases with increasing acid concentration) as follows:

$$PbO_2 + H_2SO_4 \rightarrow PbSO_4 + H_2O + 1/2O_2 \quad (2.12)$$

$$Pb + H_2SO_4 \rightarrow PbSO_4 + H_2 \quad (2.13)$$

For most positives, the formation of $PbSO_4$ by self-discharge is slow, typically much less than 0.5%/day at 25°C. The self-discharge of the negative is mainly more rapid, especially if the cell is contaminated with various catalytic metallic ions. For instance, antimony lost from the positive grids by corrosion can diffuse to the negative, where it is deposited, resulting in a ''local action'' discharge cell which converts some lead active material to $PbSO_4$. New batteries with lead-antimony grids lose about 1% of charge per day at 25°C. However, the charge loss increases by a factor of 2 to 5 as the battery ages. Batteries with non-antimonial lead grids lose less than 0.5% of charge per day regardless of age.

2.2.4.9 Temperature Effects

The VRLA batteries tend to be more susceptible to degradation aging at higher temperatures than vented lead-acid batteries. The recombination process that allows these batteries to operate without the need for periodic water addition also generates heat. Some VRLA installations may have the cells tightly packed, limiting heat dissipation capability. All of these factors combine to cause the VRLA battery to operate at higher than ambient temperature, thereby

decreasing battery life. Higher temperature will also increase the possibility of dryout and susceptibility to thermal runaway.

2.2.4.10 Ripple Current

The direct current (DC) depends on the magnitude and frequency, this superimposed ripple can produce additional heating. VRLA cell appear to be more sensitive to the heating effect because of their lower heat transfer coefficient compared to vent cells. A higher internal temperature in cells contributes to a decrease in expected service life.

2.2.4.11 Electrolyte Specific Gravity

By design, absorbed electrolyte VRLA cells have lower volumes of electrolyte than vented cells containing. If AGM cells had the same specific gravity of electrolyte as vented cells, they wound exhibit lower long-duration capacities. In gelled electrolyte cells, gel interferes with electrolyte diffusion and convection, which results in reduced high-rate capacities. In both case, the expected reductions in capacity may be partially compensated by increasing the specific gravity of electrolyte. The higher specific gravity results in higher capacity per unit volume. It also increases chemical activity and causing an increased positive plate corrosion rate. An increased corrosion reduces the service life of the cell.

2.2.4.12 Charging Voltage

Float Voltage

The actual flat voltage depends upon the specific gravity of the electrolyte being used. The recommended float voltage is provided by battery manufacture. This voltage is sufficient to keep the battery fully charged without causing excessive positive grid corrosion or forcing the battery to draw more current than is required to maintain a charge.

Temperature Compensation of Charging Voltage

Temperature-compensated charging is any method of adjusting the output voltage of the battery charger to compensate for deviations in the battery operating temperature above or below a standard value, typically 25 °C (77 °F). Owing to VRLA batteries are much more susceptible to thermal runaway than vented cell temperature-compensated charging is strongly recommended when they are used in the constant voltage float charge regime. [25-28]

2.3 Battery Definitions

2.3.1 Capacity

The capacity of a battery is the total amount of electrical energy available from a fully charged cell or cells. Its value depends on the discharge current, the temperature during discharge, the final (cut-off) voltage, and the general history of the battery. Capacity, expressed in ampere-hours (Ah) is the product of the current discharged and the length of discharge time. The nominal or rate capacity of battery (C_t) is often referred to different durations. The current is expressed as multiple of capacity:

$$C = I\Delta t$$

With I = current in Ampere

C = capacity in ampere-hour (Ah)

Δt = charge or discharge period

Rated capacity (“*C*”) is the discharge capacity which may be obtained at a given discharge rate and temperature.

C-rates specify is charge and discharge currents. At 1C, the battery charges and discharges at a current that is par with the marked Ah rating. At 0.5C, the current is half, and at 0.1C, it is one tenth. On charge, 1C charges a good battery in about one hour, 0.5C taking 2 hours and 0.1C taking10 to 14 hours.

2.3.2 Cycling, Depth of Discharge (DOD)

Batteries based on chemical reactions and involved components undergo substantial changes during discharging and charging. The number of discharging/charging cycles and the depth of discharge (DOD) influence service life significantly. The relation between depth of discharge and the achieved cycle numbers for VRLA battery was shown in Figure 2.6.

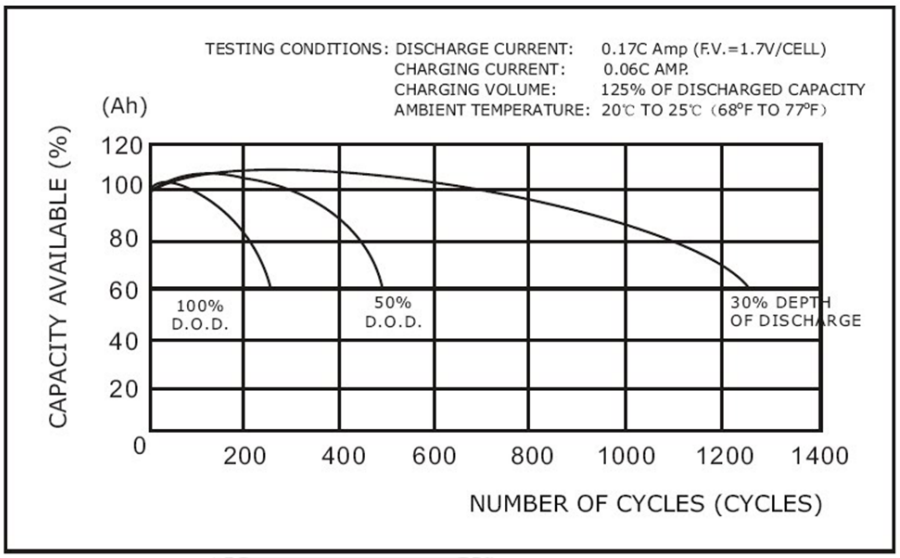

Figure 2.6 Cycle service life in relation to depth of discharge for VRLA battery

2.3.3 Deep Discharge

Conventional batteries are destroyed by deep discharging, because the solubility of lead ions increases in the diluted electrolyte. Failure occurs by the formation of short circuits that are caused by the precipitation of lead dendrites during charging. By contrast, VRLA Batteries are extremely resistant to deep discharging. In some specifications, a 4-week deep-discharge performance at the 5-h rate is required.

2.3.4 Voltage

The imprinted voltage refers to the nominal battery voltage. The correct voltage has been observed when battery connects to a load or a charger. If the voltage differs, the process must not be done. The open circuit voltage (OCV) on a fully charged battery can be slightly higher than the nominal. The closed circuit voltage (CCV) represents the battery voltage under load or on charge, and the readings will vary accordingly.

2.3.5 Specific Energy and Energy Density

Specific energy or gravimetric energy density indicates the battery capacity in weight (Wh/kg). Energy density or volumetric energy density is given in size (Wh/l). For the case in an alkaline battery, specific energy of battery is high while specific power is poor (load capability). Alternatively, a battery may have a low specific energy but it can deliver high specific power, as is possible with the supercapacitor. Specific energy is synonymous with battery capacity and runtime.

2.3.6 Specific Power

Specific power or gravimetric power density shows the loading capability, or the amount of current the battery can provide. Battery for power tools exhibits high specific power but it has reduced specific energy (capacity). Specific power is synonymous with low internal resistance and the delivery of power.

2.3.7 Self-discharge

Due to the usage of an antimony-free alloy with a high hydrogen overvoltage, VRLA batteries have a low self-discharge. After two years storage at 25 °C, the residual capacity is at least 75%. This corresponds to a daily self-discharge rate of 0.08%.

2.3.8 Service Life

The service life of battery is necessarily limited and life expectancy an important question. Service life is judged differently, depending on the application of battery. For standby batteries, which are only rarely discharged, service life expressed in calendar time is important parameter. For other applications, service life is characterized by the possible of discharging/charging cycles [29].

2.4 Gelled Electrolyte Immobilization with Fumed Silica (Pyrogenic Silica)

Figure 2.7 Powder of Fumed Silica

Fumed silica is very fine dispersed SiO_2 powder, particle size 5-50 nm, surface area 50-600 m^2/gram. Fumed silica is formed by injecting chlorosilanes, such as silicon tetrachloride, into a flame of hydrogen and air at temperature above 1500 $^{\circ}C$. Fumed silica and hydrogen chloride are the product of this reaction. The SiO_2 molecules strongly bond in siloxane groups (Si-O-Si) bind together to sphereical primary particles of 10 nm particles. As the particle moves to colder areas, they bind together to form a chain like aggregates with length up to approximately 1μm. After further cooling, form the agglomerates with a diameter of 10 to 250 μm. The boding force between primary particles is hydrogen linkage. The silanol groups (Si-O-H) of two particles come in contact and create the bridge linkage by exchanging their hydrogen atom.

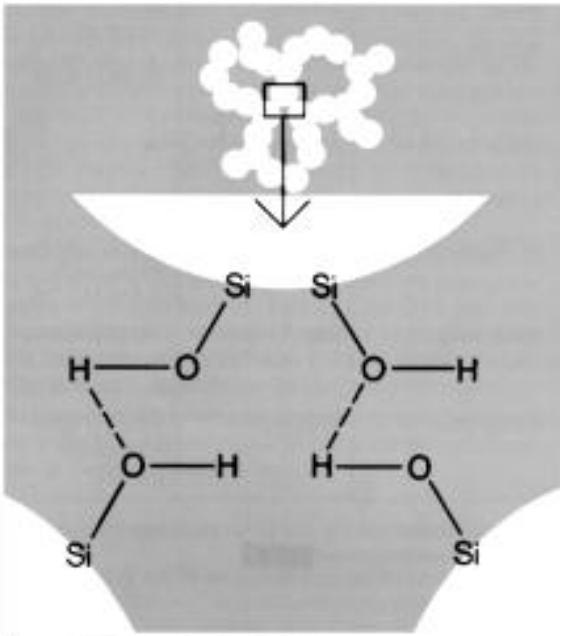

Figure 2.8 Hydrogen bridge linkages between particles [30].

These agglomerated aggregates of SiO_2 particles are mixed with acid and water, forming a liquid GEL (SOL). A silica particle gel or a sol will form in sulfuric acid solution as colloid silica gel after dispersed (Figure 2.9). The sulfuric solution is a weak hydrogen-bonding, aqueous media because the SO_4^{2-} ion plays a steric hindrance role. The silica particles are envisioned to interact directly with each other through hydrogen bonding interactions between the surface silanol (Si-OH) groups. It is believed that hydrogen bond interactions are responsible for the gelled formation, not Van der Waals interactions. Therefore, a uniform distribution of silica particle in sulfuric acid would help to optimize the interaction of surface silanol (Si-OH) groups on the silica particles, resulting in the formation of the uniform, microscopic, three-dimensional gel structure, which provides the gel with high capacity and low inner resistance.

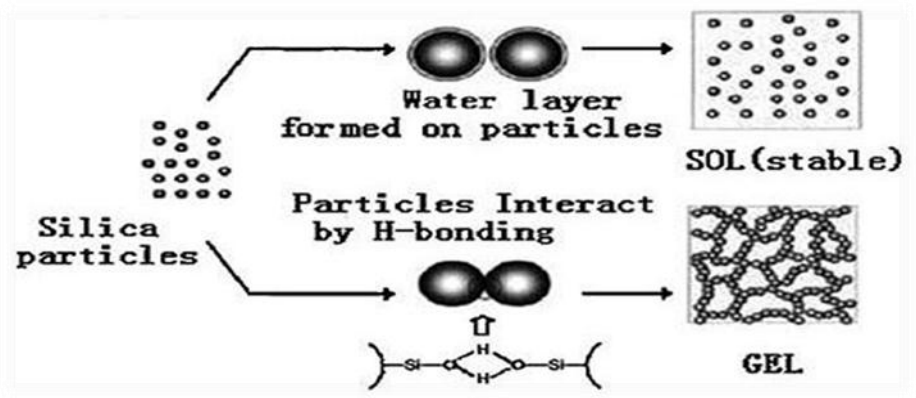

Figure 2.9 Interaction effect of solvent between fumed silica particle : (a) strongly hydrogen bonding liquid (b) a weakly hydrogen bonding [31]

After several hours of setting, the hydrogen bridge linkages form a three-dimension structure. This is the GEL, seen in the right hand side of Figure 2.10. The most important information is that sulfuric acid solution are trapped in this structure, which is formed by chains with a diameter of only 10 nm or 0.02 μm.

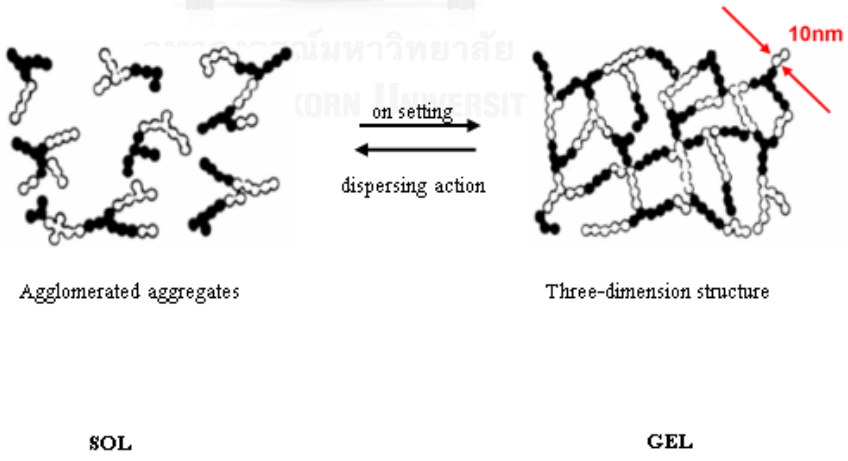

Figure 2.10 The formation of GEL structure is reversible at the beginning by dispersing SOL and by setting GEL [30].

2.5 Additives

2.5.1 Graphene

Graphene (GP) is a monolayer, crystalline allotrope of carbon which is densely packed in a regular sp^2-bonded atom into a two dimensional honeycomb lattices. It has been adopted an attractive material since it was discovered in 2004 by Andre Geim and Kostantin Novoselov [10, 13]. Graphene is a unique material because of its mechanical, electrical and optical properties (Figure 2.11). GP also has the strong carbon/carbon bonding in the flat, aromatic structure, π electrons, and reactive sites for surface reactions.

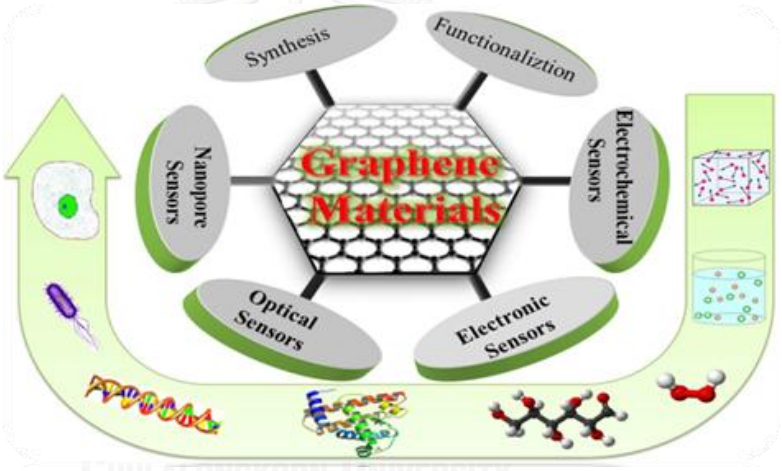

Figure 2.11 Various application of graphene

Furthermore, GP has become an outstanding nanomaterial in electrochemistry [9-12] due to good chemical stability, high electrical and thermal conductivity, excellent mechanical properties, and large surface area. However, GP shows high tendency to agglomerate and restack to form graphite through p–p stacking and Vander Waals interactions which make the use of GP is limited in some applications [14, 15].

2.5.2 Polyvinylpyrrolidone (PVP)

Polyvinylpyrrolidone (PVP), a linear homopolymer of N-vinylpyrrolidone, is widely used in pharmaceutical science and food applications. PVP is soluble in water and other polar solvents. The advantages of PVP are low cost and biocompatibility. Moreover, there is research reported on the application of PVP to successfully stabilize the dispersion of graphene at high concentration in organic solvents [32, 33]. The structure of PVP is shown in Figure 2.12.

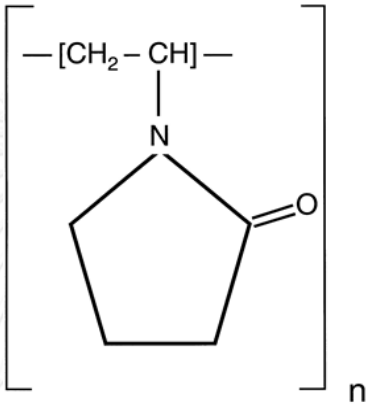

Figure 2.12 Structure of Polyvinylpyrollidone (PVP)

2.5.3 Polyaniline

Conducting polymers, specifically polyaniline (PANI), poly (3,4-ethylenedioxythiophene) (PEDOT) and polypyrrole (PPy), have been extensively studied and widely applied in various electrochemical device storage. Among various the conductive polymers, polyaniline (PANI) is considered as one of the most useful conducting polymers because of its environmental stability, ease of synthesis, and simple doping/dedoping chemistry [17-19, 34]. The structure of PANI is shown in Figure 2.13.

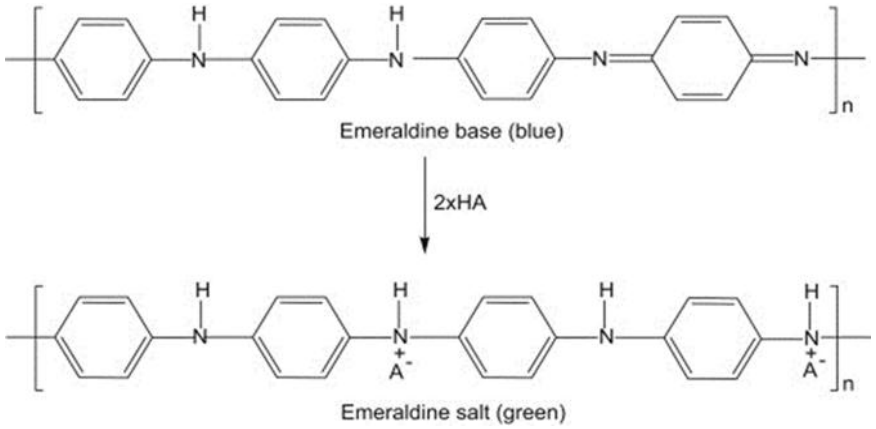

Figure 2.13 Structure of PANI doping/depoing)

2.6 Electrochemical Technique

2.6.1 Cyclic Voltammetry

Cyclic voltammetry is one of the electroanalytical methods which measure the current as a function of the applied potential. Three electrodes are used in this method, including working electrode, counter electrode, and reference electrode. For this technique, at static working electrode (unstirred solution) was applied potential both forward and reverse directions as shown by the waveform in Figure 2.14 a. The current is measured by the potentiostat instrument while the potential sweep is applied. For the results of cyclic voltammetry, the current and potential are plotted as called cyclic voltammogram. Figure 2.14 b showed the cyclic voltammogram of a reversible redox couple. Clyclic voltammogram is characterized by peak potential (E_p) where E_{pa} and E_{pc} are anodic and cathodic peak potential, respectively. The i_p is the maximum current value where i_{pa} and i_{pc} are anodic and cathodic peak current, respectively [35].

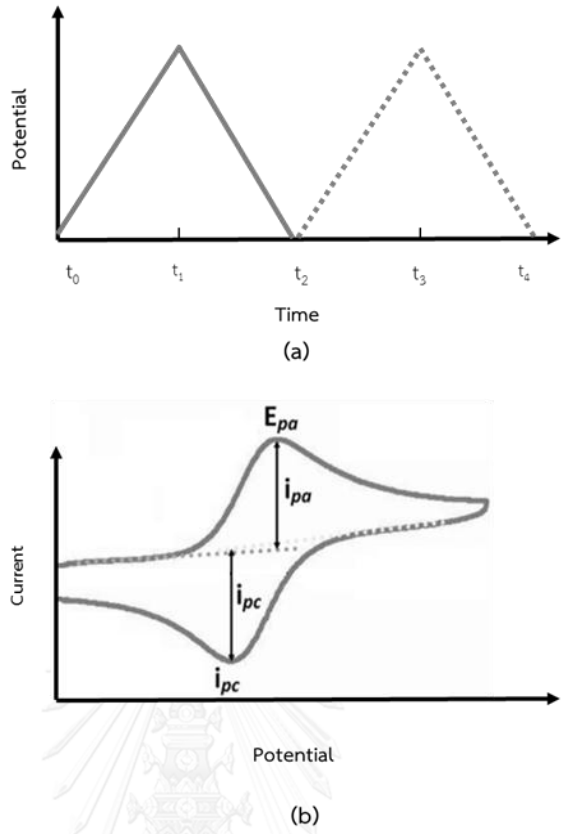

Figure 2.14 Waveform of cyclic voltammetry (a) and cyclic voltammogram of reversible redox couple (b) [36]

2.6.2 Electrochemical Impedance Spectroscopy (EIS)

Electrochemical impedance is based on applying an alternating potential, a sinusoidal potential excitation to an electrochemical cell and then measuring the current through the cell. The obtained current is an alternating current (AC) signal, which can be analyzed as a summation of sinusoidal functions.

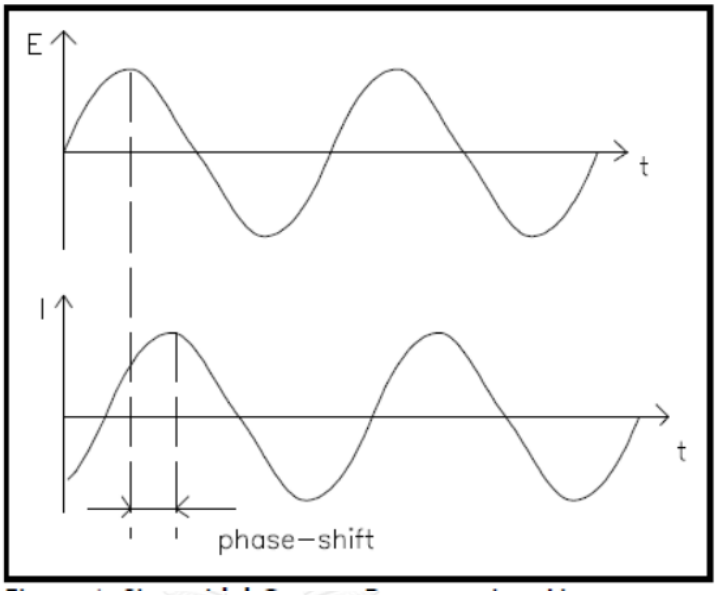

Figure 2.15 Sinusoidal current response in a linear system

The excitation signal is expressed as a function of time;

$$E_t = E_0 \sin(\omega t) \tag{2.14}$$

Where E_t is a potential at time t, E_0 is amplitude of an excitation signal, and ω is a radial frequency. The relationship ω (expressed in radians/second) and frequency f (expressed in hertz) is shown as the following equation:

$$\omega = 2\pi f \tag{2.15}$$

The response current signal is expressed as a following function with phase shift (ψ) and a different amplitude, I_0 :

$$I_t = I_0 sin(\omega t + \emptyset) \tag{2.16}$$

The impedance (Z) of system is calculated by an expression analogous as following equation:

$$Z = \frac{E_t}{I_t} = \frac{E_0 sin(\omega t)}{I_0(\omega t + \emptyset)} = Z_0 \frac{sin(\omega t)}{sin(\omega t + \emptyset)} \tag{2.17}$$

The impedance is therefore expressed in terms of a magnitude, Z_0, and ψ. If the applied potential (E_t) and response current (I_t) are plotted on x-axis and y-axis, respectively as shown in Figure 2.15. The oval in the Figure 2.16 is known as "Lissajous Figure". Analysis of Lissajous Figures on oscilloscope screens was the accepted method of impedance measurement prior to the availability of modern EIS instrumentation.

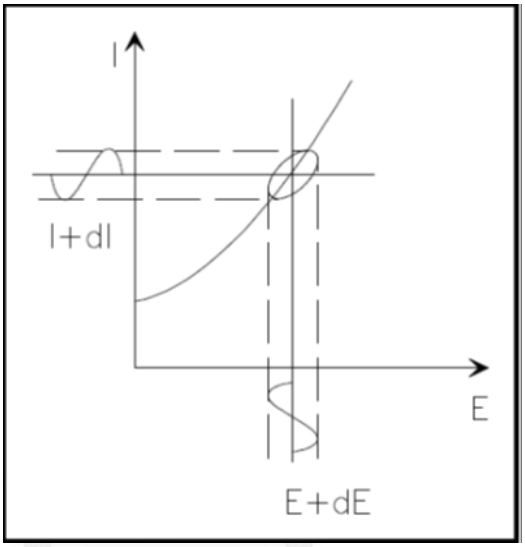

Figure 2.16 Origin of lissajous figure

With Eulers relationship,

$$\exp(j\emptyset) = \cos\emptyset + j\sin\emptyset \tag{2.18}$$

It is possible to express the impedance as a complex function. The potential is described as,

$$E_t = E_0\exp(j\omega t) \tag{2.19}$$

And the current response as,

$$I_t = I_0\exp(j\omega t - \emptyset) \tag{2.20}$$

The impedance is then represented as a complex number,

$$Z(\omega) = \frac{E}{I} = Z_o\exp(j\emptyset) = Z_0(\cos\emptyset + j\sin\emptyset) \tag{2.21}$$

Data Presentation

From the equation 2.21, the expression for Z (ω) is composed of a real and an imaginary part. If the real part is plotted on the X-axis and the imaginary part is plotted on the Y-axis of a chart, "Nyquist Plot" is obtained (see Figure 2.17). In this plot, the Y-axis is negative and each point on the Nyquist Plot is the impedance at one frequency (data are on the right side of the plot and higher frequencies are on the left).

On the Nyquist Plot, the impedance can be represented as a vector (arrow) of length |Z|. The angle between this vector and the X-axis, commonly called the "phase angle", is ψ (=arg Z).

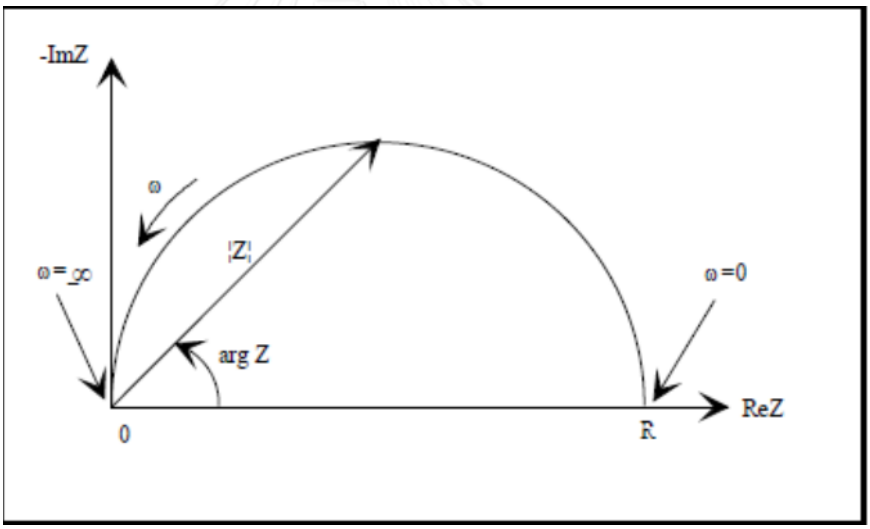

Figure 2.17 Nyquist Plot with Impedance Vector

Nyquist Plots have one major shortcoming. It cannot tell what frequency was used to record that point.

The Nyquist Plot in Figure 2.17 results from the electrical circuit of Figure 2.18. The semicircle is characteristic of a single "time constant". Electrochemical impedance plots often contain several semicircles. Only a portion of a semicircle is often seen.

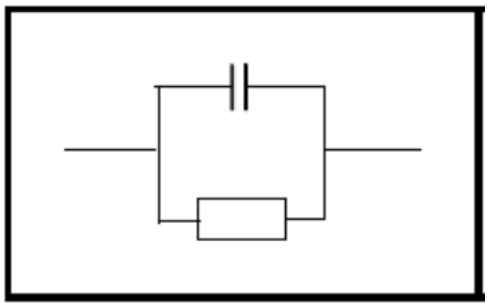

Figure 2.18. Simple equivalent circuit with one time constant

Another popular presentation method is the Bode Plot. The impedance is plotted with log frequency on the X-axis and both the absolute values of the impedance (|Z|=Z0) and the phase-shift on the Y-axis. The Bode Plot for the electric circuit of Figure is shown in Figure 2.18. Unlike the Nyquist, the Bode Plot does show frequency information. [37]

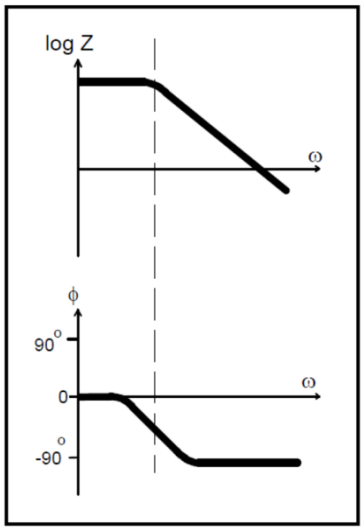

Figure 2.19 Bode plot with one time constant

2.7 Literature Review

In 1995, Dietz *et al*. [38] studied the influence of substituted benzaldehydes and their derivatives as inhibitors for hydrogen evolution on negative electrodes of the lead/acid. The system was investigated by cyclic voltammetry. The result was found that the substituted benzaldehydes and their derivatives can reduce the water

loss in flooded lead acid batteries during cycling about 50% comparing to batteries without additive.

In 2006, Karimi *et al*. [39] studied the effect of sodium sulfate as negative paste additive on performance of lead acid batteries. From the results, batteries containing 0.1% (wt) sodium sulfate exhibited the highest effectiveness which the discharge capacity increased more than 3%, the time of 6V at cold cranking test increased more than 17%, the cycle life of the lead-acid batteries increased more than 18%.

In 2008 Chayasit *et al*. [40] studied the effect of various additives in gel electrolyte, including polyaniline, polypyrrole, sodium sulfate, and potassium sulfate, on performance of lead acid batteries. The investigation was done by measuring the conductivity value and discharge capacity. The results indicated that the addition of polypyrrole in gel electrolyte exhibited the highest discharge capacity. This research was studied independently similar and complementary investigation by Chaiyasit *et al*. Additionally, this work was concentrated on the use of GP-PANI with different conditions, and long-term stability of battery performance.

In 2008, Siridetpan [41] developed the gelled electrolyte in valve-regulated lead-acid (VRLA) battery using polyacrylamide, sodium sulfate, magnesium sulfate, and potassium sulfate. The conductivity was used to study the electrochemical behavior of gelled electrolyte. The results showed that polyacrylamide exhibited highest conductivity, gel strength, and the gelling time. On the other hand, sodium sulfate displayed the lower conductivity. For the performance of gel VRLA battery, sodium sulfate provided the longest discharging period, the highest discharge capacity.

In 2009, Pavlov *et al*. [42] studied the effect of different particle size of carbon (electrochemically active carbons) as additive on negative electrode. The results indicated that the electrochemically active carbons (EAC) exhibited a highly

catalytic effect on the charge reaction. Consequently, the reversibility of the charge/discharge processes improved, which eventually leads to longer battery cycle life.

In 2011, Tantichanakul *et al*. [7] studied the effect of veratraldehyde as an additive in gelled electrolyte. The electrochemical behavior and performance of AGM VRLA batteries were investigated. The result was found that veratraldehyde could suppress the hydrogen evolution reaction. The addition of 0.005% (w/v) veratraldehyde further improved battery performance better than conventional nongel AGM VRLA batteries.

In 2012, Pan *et al*. [43] prepared and investigated a novel gelled electrolyte using the combination between colloidal and fumed silica. The physical property testing demonstrated that the mixed gel electrolyte was more mobile, had a longer gelling time, greater stability and a better crosslinking structure than its counterparts as compared with any single gelling agent. The electrochemical properties indicated that mixed gel electrolyte could suppress the oxygen evolution reaction, reduce the resistance to charge transfer at open circuit potential, increase the initial capacity, demonstrating that it is a promising gel electrolyte for lead acid batteries.

CHAPTER III

EXPERIMENTAL

3.1 Chemicals

Table 3.1 List of chemicals for the preparation of gelled electrolyte

Chemicals	Suppliers
Fumed silica (Aerosil 200) Particle size 12 nm BET surface area 200±25 $m^2 g^{-1}$	Dugussa (Essen, Germany)
Sulfuric acid 95-97%	Merck (Darmstadt, Germany)
Polyaniline (PANI)	Sigma-Aldrich (State of Missouri, USA)
Polyvinylpyrrolidone (PVP)	Sigma-Aldrich (State of Missouri, USA)
Camphor-10-sulfonic acid (CSA)	Sigma-Aldrich (State of Missouri, USA)
Chloroform ($CHCl_3$)	Merck (Darmstadt, Germany)
Dimethylformamide (DMF)	-
Graphene (GP) powder	Sky Spring Nanomaterials, Inc. (Texas, USA)

3.2 Preparation of Additives

Firstly, PANI was doped with CSA to generate a conductive form of PANI and dissolved in chloroform. The solution was then stirred and filtrated, and the green solution was ready to use (Figure 3.1a). For the preparation of GP and GP-PVP solution, 200 mg of GP powder was added into 100 mL of dimethylformamide

(DMF), and GP powder and polyvinylpyrrolidone (PVP) were added into DMF, respectively. Both GP and GP-PVP solution were then sonicated for 6 hr at room temperature. The solutions of GP and GP-PVP were shown in Figure 3.1b and Figure 3.1c, respectively. After that, the solution of PANI was added into the dispersed GP and GP-PVP, respectively. Finally, the mixture solution of graphene-polyaniline composite (GP-PANI) and GP-PVP-PANI were obtained.

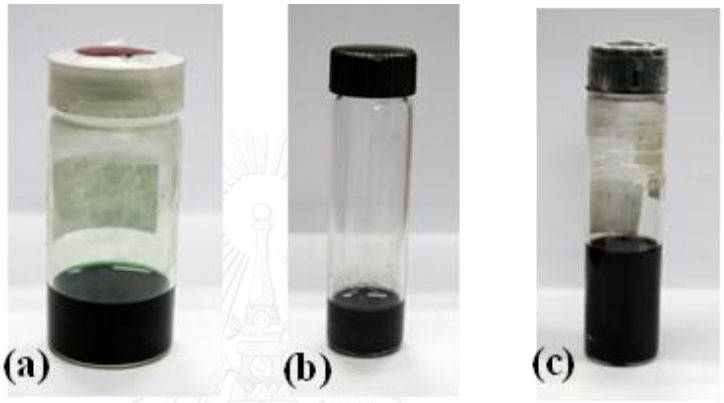

Figure 3.1 Additives for modification of gelled electrolyte including (a) polyaniline (PANI) (b) graphene (GP) (c) graphene with polyvinylpyrrolidone (GP-PVP)

3.3 Preparation of Gelled electrolyte

3.3.1 Instrument

Gelled electrolyte was prepared using POLYTRON® PT3100 as a mixing machine (supplies by KINEMATICA AG Switzerland) as shown in Figure 3.2.

Figure 3.2 The setting of instrument for the gelled electrolyte preparation

3.3.2 Methodology

The gelled electrolyte was prepared using fumed silica particle, sulfuric acid, additive, and distilled water. The various contents of fumed silica were first mixed with diluted sulfuric acid solution. Next, the additive was added to the mixtures. The mixtures were dispersed using a homogenizer with speed of 3,000 rpm for 10 min at room temperature to allow the formation of gelled electrolyte as shown in Figure 3.3.

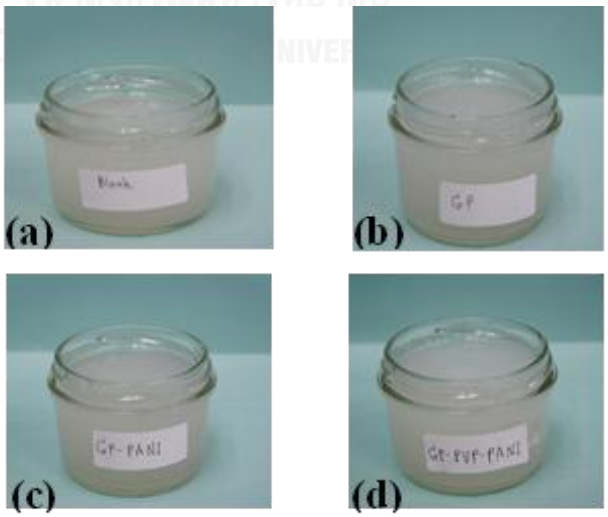

Figure 3.3 Composition of gelled electrolyte in (a) the absence of additive, and (b) the presence of GP, (c) GP-PANI, and (d) GP-PVP-PANI

3.4 Gel time and Gel hardness Test

3.4.1 Instrument

Figure 3.4 Instrument for gel time and gel hardness test

Table 3.2 List of instruments for gel time and gel hardness test

Instruments	Detail
Lead ball	3 mm, 0.3g
Timer	-
Test tubes	(16×150mm)
Metric ruler	(>15cm, accuracy +/- 1mm)
Test tube rack	-
Beakers	800 ml or comparable volume
Balance	range 10,000g +/- 0.1g
Thermometer	with range 0 to 100 ℃ ±0.5℃

3.4.2 Methodology

The dispersed fumed silica in sulfuric acid was filled into the test tubes. In order to investigate the gelling time, the lead ball was dropped from specified height into test tube contained gelled electrolyte every 15 minute until 7 hour (Figure 3.4). After optimization, the optimal gelled electrolyte formula with suitable gelling times (longer than 3 hour) was then selected to fill into the 12 V/7 A AGM VRLA batteries using filling machine under a vacuum condition. Only the gelled electrolyte formulation maintained a liquid state before filling in the batteries was chosen.

3.4.3 Gelled Electrolyte for Gel Time and Gel Hardness Test

The optimal concentration of fumed silica was investigated by gel time and gel hardness test. The composition of gelled electrolyte for this test included 3-5% (w/v) of fumed silica and 43%w/v of sulfuric acid (1.325 sp.gr.) was shown in Table 3.3. Then, this composition was mixed using homogenizer with speed of 3,000 rpm for 10 min at room temperature.

Table 3.3 List of gelled electrolyte without additive for gel time and gel hardness test

Fumed silica content (%w/v)	H_2SO_4 (sp.gr.)
3	1.325
4	1.325
5	1.325

3.5 Electrochemical Test

3.5.1 Instrument

In this work, the electrochemical characterization was investigated including cyclic voltammetry (CV) and electrochemical impedance spectroscopy (EIS). Both methods were performed using the potentiostat (PGSTST 30) containing with three-electrodes system.

(a) (b)

Figure 3.5 The electrochemical cell for electrochemical technique. (a) potentiostat (PGSTST30) (b) planar Lead (Pb) electrode

Table 3.4 List of instruments for electrochemical test

Instruments	Detail	Supplies
Potentiostat (PGSTST30)	Auto lab	Metrohm
Planar Lead (Pb)electrode	WE electrode	Homemade
Platinum gauze 80 mesh	CE electrode	BAS Inc.
Ag/AgCl electrode	RE electrode	Metrohm

3.5.2 Cyclic Voltammetry (CV)

3.5.2.1 Methodology

To investigate the hydrogen-oxygen evolutions, cyclic voltammetry (CV) using PGSTAT 30 (Auto lab, Eco Echemie BV company) was

performed by three-electrode system including Ag/AgCl as a reference electrode, 1 cm^2 planar lead (Pb) as a working electrode, and a platinum guaze as a counter electrode. CV curves were recorded in the potential range from -2.0 to 2.9 V at scan rate of 50 mVs^{-1} to investigate the evolution of hydrogen and oxygen . At the beginning in each experiment, the working electrode (Pb) was mechanically polished using water-resistant emery paper and washed with distilled water.

3.5.2.2 Gelled electrolyte for Cyclic Voltammetry

Gelled electrolyte was used to study hydrogen-oxygen evolution, including 3-5% (w/v) of fumed silica and 43% (w/v) sulfuric acid solution (1.325 sp.gr.) as shown in Table 3.5. These compositions were mixed by homogenizer and filled into the bottle. After that, the compositions were kept for 1 week to set completely gelled electrolyte, and then cyclic voltammetry was measured.

Table 3.5 List of gelled electrolyte without additive for investigation of the hydrogen-oxygen evolutions using cyclic voltammetry

Fumed silica content (%w/v)	H_2SO_4 (sp.gr.)
3	1.325
4	1.325
5	1.325

3.5.3 Electrochemical Impedance Spectroscopy (EIS)

3.5.3.1 Methodology

Similarly to the cyclic voltammetry, three-electrode system was used in the EIS measurements. Ag/AgCl was used as a reference electrode, 1 cm^2 planar lead (Pb) was used as a working electrode, and a platinum guaze was used as a counter electrode. The condition of EIS method was operated under the frequency in the range of 10^5 to 10^{-2} Hz at amplitude 10 mV. At the beginning of each experiment, the working electrode (Pb) was mechanically polished using water-resistant emery paper and washed with distilled water.

3.5.3.2 Gelled electrolyte for Electrochemical Impedance Spectroscopy (EIS)

Gelled electrolyte was used to investigate charge transfer resistant by EIS, including 4% (w/v) of fumed silica, 43% (w/v) of sulfuric acid solution (1.325 sp.gr.), and the different concentrations of additives. The gel electrolytes were classified into four types, consisting of (i) without additive, (ii) adding GP, (iii) adding GP-PANI, and (vi) adding GP-PVP-PANI as shown in Table 3.6. These compositions were mixed by homogenizer and filled into the bottle. After that, the compositions were kept for 1 week to set completely gelled electrolyte, and then EIS measurement was performed.

Table 3.6 List of gelled electrolyte in the presence and absence of additive

Fumed silica content (%w/v)	H_2SO_4 (sp.gr)	Concentration of additive (mgL^{-1})	Type of additive
4	1.325	0	Without additive
4	1.325	5	GP,GP-PANI,GP-PVP-PANI
4	1.325	10	GP,GP-PANI,GP-PVP-PANI
4	1.325	20	GP,GP-PANI,GP-PVP-PANI
4	1.325	40	GP,GP-PANI,GP-PVP-PANI
4	1.325	60	GP,GP-PANI,GP-PVP-PANI

3.6 Battery Test

The optimal gelled electrolyte which exhibited from lowest charge transfer resistant from EIS, was chosen for battery test. The gelled electrolyte was added into the 12V/7A battery using the filling machine. Charge-discharge capacity was tested to investigate the performance of cycling battery.

3.6.1 Instrument

Instrument for investigation of the performance of battery with the different additives in gel electrolyte was shown in Figure 3.6.

Figure 3.6 Battery charge/discharge and data processing control system (Xin Ke Hua Industry Co., Ltd)

3.6.2 Methodology

To test the performance of the batteries, the discharge capacity was measured at 25±2 °C during 190 cycles. All batteries were charged by constant current at 2 A within 9 hr. The discharged current was 7 A, and cut-off voltage was 9.6 V as shown in Table 3.7.

Table 3.7 Summarized cyclic test algorithms used in the battery tests under a 100% depth of discharge (DoD).

Step	100% DoD
	Cycle life test (1C)[a]
1	Charge (2 A/14.1 V/9 hr)
2	Rest(5 hr)
3	Discharge (7 A/9.6 V)
4	Charge (2 A/14.1 V/9 hr)
5	Repeat step 3 and 4 189 times

3.7 Scanning Electron Microscopic (SEM) Analysis

3.7.1 Instrument

Instrument obtained from JEOL scanning electron microscope JSM 6400 was used for scanning electron microscopic (SEM) analysis.

3.7.2 Methodology

After the study of discharge capacity of 12 V/7A VRLA battery was accomplished, the negative plate electrode (Pb) was separated and trimmed to cubic shape, and then the trimmed Pb electrode was allowed to dry at room temperature for 48 hr. The morphology of the trimmed negative plate electrode (Pb) was observed using SEM analysis.

3.8 Transition Electron Microscopic (TEM) Analysis

3.8.1 Instrument

Instrument obtained from JEOL scanning electron microscope JEM-2100 was used for transition electron microscopic (TEM) analysis.

3.8.2 Methodology

Morphology of additives, mixtures of additive, and gel electrolyte was studied using TEM analysis. Grid, which supported substrate for TEM analysis, was dipped in the GP, GP-PANI, and GP-PVP-PANI additives, and allowed it to dry within 24 hr at room temperature. After obtained TEM image, the morphology and nanostructure of GP, GP-PANI, and GP-PVP-PANI additives were observed.

3.9 Fourier Transform Infrared Spectroscopy (FTIR) Analysis

3.9.1 Instrument

Fourier transform infrared spectroscopy (Nicolet 6700) instrument was obtained from Nicolet, USA. The FTIR conditions consisted of a frequency of 400-4000 cm-1 using TGS detector with 32 scans at resolution 4 cm^{-1}.

3.9.2 Methodology

GP, GP-PANI, and GP-PVP-PANI additives were studied using FTIR analysis for identification of functional group. These additives were suspended and freeze-dried, respectively. The FTIR spectrum was recorded in KBr discs.

CHAPTER IV

RESULTS AND DISCUSSION

4.1 Characterization of Additive

The morphology of the GP-PANI was characterized using transition electron microscopy (TEM) as shown in Figure 4.1. It was found that, TEM image of GP-PANI with electron diffraction pattern of GP as shown in insert of Figure corresponding to the previous report [42]. This image indicated that a good dispersion of GP-PANI was obtained without severe aggregation.

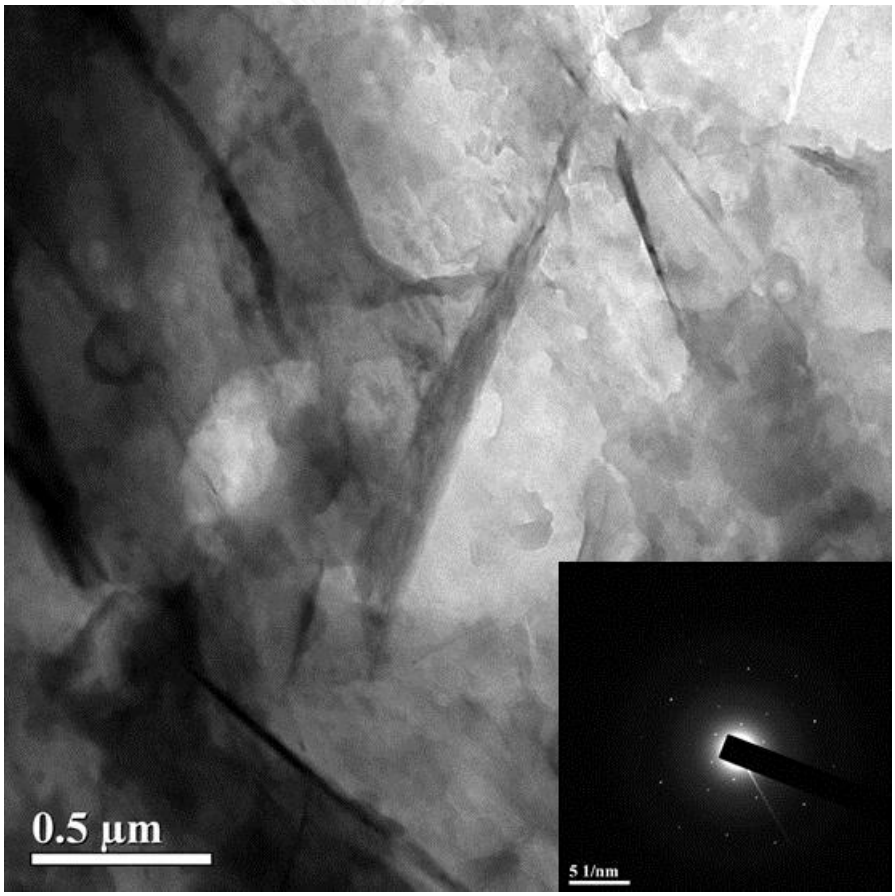

Figure 4.1 TEM image of GP-PANI additive added in gelled electrolyte, (inset) the electron diffraction pattern of GP

4.2 Characterization of Gelled Electrolyte

The gelling times were investigated by measuring the distance of penetration by dropping 3 mm lead balls into the test tube containing gelled electrolyte. The gelling time was observed by visualization as shown in Figure 4.2. Those gelled electrolyte formulas with suitable gelling times (longer than 3 hour) were then selected to fill into the 12 V/7 A AGM VRLA batteries.

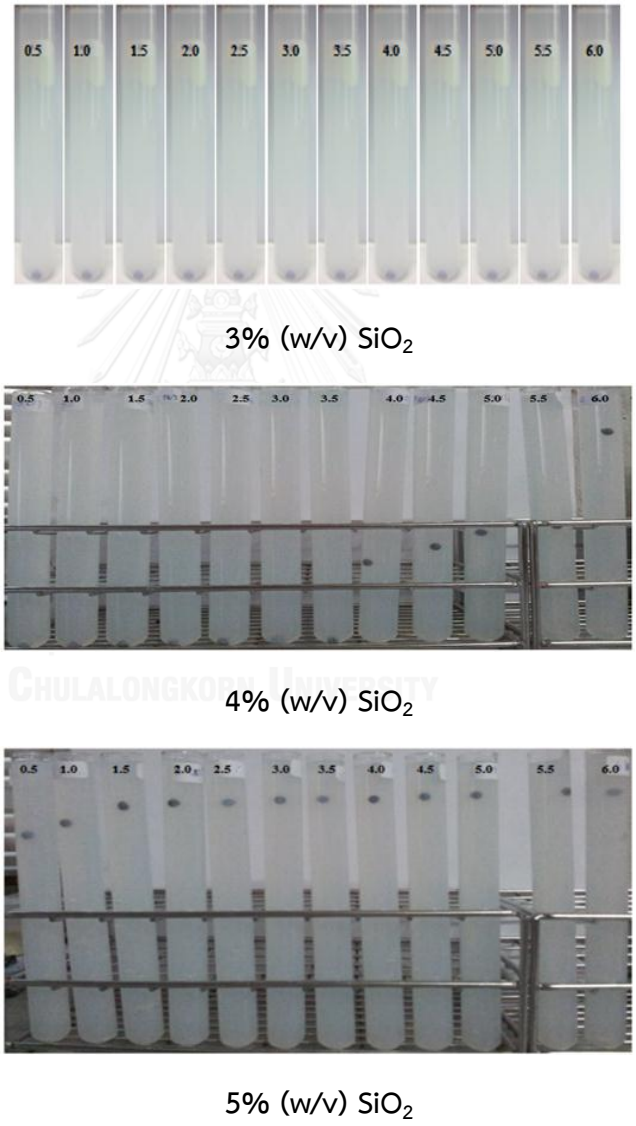

Figure 4.2 Photographs of lead balls dropped in gelled electrolyte at various times and SiO_2 concentrations.

The gel time and gel hardness were plotted between depth of penetration and time. During the electrolyte filling process, there are three major factors consisting of stability, strength and gelling time. The penetration of the dropped lead balls into the gel electrolytes (the representative measurement of gel firmness and strength) at various times is demonstrated in Figure 4.3. The gelling time reduced and the gel strength increased when the fumed silica (SiO_2) concentration increased from 3 to 5% (w/v). From the results, the electrolyte contained with 3% (w/v) SiO_2 was too dilute, and gel structure could not form even though setting more than 6 hour. Therefore, it was not suitable for filling into batteries. The electrolyte contained with 4% (w/v) SiO_2 start to form gel after 3 hour, so gel structure did not form before filling into batteries, which is required condition. For the electrolyte with 5% (w/v), gel structure formed rapidly within 30 minute, so it was hardly filled into batteries. In addition, it has been reported that the higher SiO_2 concentration lead to the formation of a greater silanol-bonding network (i.e., the network of Si–O–H through the hydrogen bridge linkages), which then resulted in a faster and firmer gelled electrolyte [5]. Therefore, 4% (w/v) SiO_2 was chosen as an optimal condition for further study.

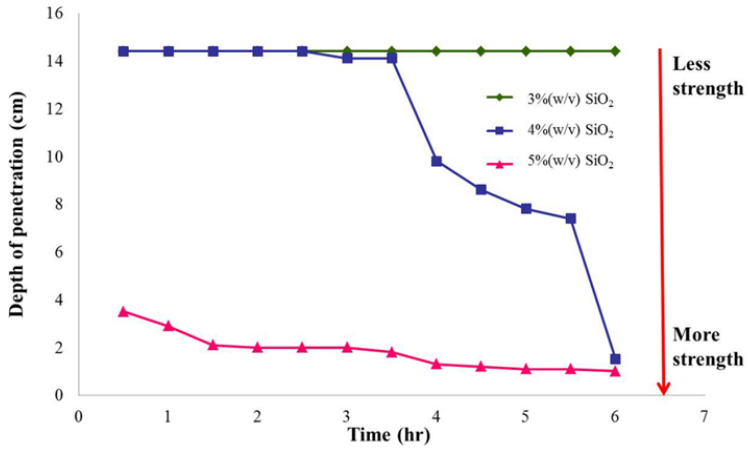

Figure 4.3 Penetration depth of lead balls dropped at different times in gelled electrolyte with different SiO_2 concentrations.

4.3 Electrochemical Test

4.3.1 Cyclic Voltammetry

To investigate the hydrogen-oxygen evolutions occurring inside gel AGM battery, cyclic voltammetry was performed with scanning potential range of -2.0 to 2.9 V and scan rate 50 mVs^{-1}. Figure 4.4 shows cyclic voltammogram of gelled electrolyte in the absence and presence of additives. The results show that the hydrogen-oxygen evolution related to the water loss in battery due to the overcharging process. The rate of hydrogen and oxygen evolution required balance, otherwise leading to the softening of positive active material (PAM) and degradation of negative plate that affect service life. The comparison between the presence and absence of additives in the gelled electrolyte of 4% (w/v) SiO_2 was investigated. For the presence of additives, GP or GP-PANI were used in gelled electrolyte. The cyclic voltammogram displayed similar peak at –0.5 V and 1.5 V, corresponding to the $Pb/PbSO_4$ and $PbO_2/PbSO_4$ reactions [1, 44] respectively. The oxidation of $PbSO_4$ to PbO_2 appeared at -0.5 V and the reduction of PbO_2 to $PbSO_4$ appeared at 1.5 V. From the redox peaks current, the hydrogen peak obtained from the presence of GP in gelled electrolyte was smaller than that one obtained from gelled electrolyte without additive. However, the oxygen peaks for both conditions were similar. After adding GP-PANI in gelled electrolyte, both hydrogen and oxygen peaks were clearly lower than without addition of additive and with adding of GP additive. Therefore, GP-PANI was chosen as the additive of gelled electrolyte for filling in AGM VRLA batteries because the hydrogen and oxygen peak are reduced. It can be concluded that the loss of water was reduced when used additive. This electrochemical behavior indicates that addition of GP-PANI additive can increase the service life of the batteries.

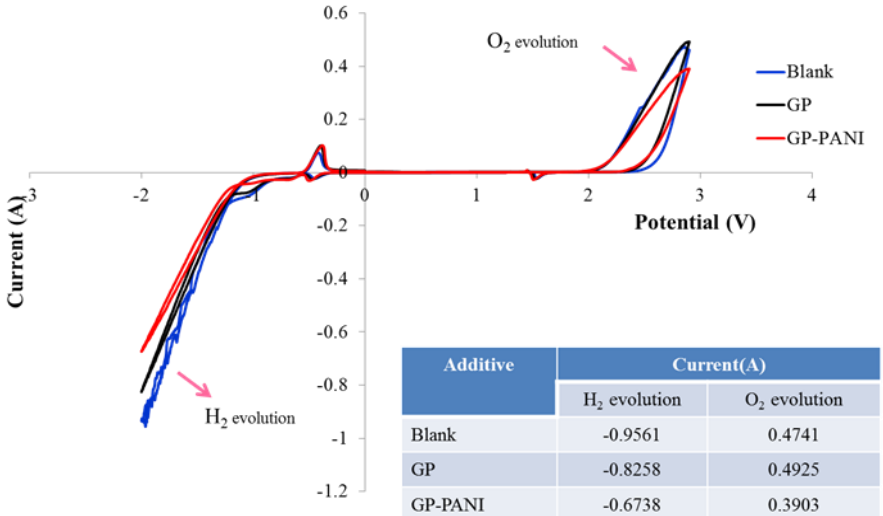

Additive	Current(A)	
	H_2 evolution	O_2 evolution
Blank	-0.9561	0.4741
GP	-0.8258	0.4925
GP-PANI	-0.6738	0.3903

Figure 4.4 Cyclic voltammograms of gelled electrolyte with different additives added to electrolyte at 50 mV s^{-1} (-2.0 to 2.9 V).

4.3.2 Electrochemical Impedance Spectroscopy

To optimize concentration of additive added in gelled electrolyte electrochemical impedance spectroscopy was used. Figures 4.5, 4.6 and 4.7 show the Nyquist impedance spectra of gelled electrolyte containing GP, GP-PANI and GP-PVP-PANI, respectively. The concentration of additive was optimized in the range of 5-60 ppm. All impedance spectra show one semicircle at high frequency (10^5 Hz). Generally, the semicircle at high to medium frequency is associated with charge transfer resistance. The low frequency is related to Warburg impedance associated with ion diffusion process at electrode material [43, 45]. In this work the absence of Warburg impedance in gelled electrolyte means that the reaction at the electrode/electrolyte interface was not controlled by ion diffusion.

The Nyquist plots for five concentrations of GP show similar one semicircle at high frequency as shown in Figure 4.5. The diameters of semicircle are related to charge transfer resistance at the electrolyte/electrode interface, the smaller diameters of semicircle, smaller charge transfer resistance and higher

conductivity. Therefore, 20 ppm of GP was chosen because of lowest diameter of semicircle, indicating that the lowest charge transfer resistance. Both Nyquist plots of GP-PANI and GP-PVP-PANI are similar. The concentration of additive at 20 ppm shows the lowest charge transfer resistance among the other concentrations as shown in Figure 4.6 and 4.7, respectively. Additionally, the gelled electrolyte which provides the lowest charge transfer resistance was GP-PANI at 20 ppm of GP and PANI as shown in Figure 4.8.

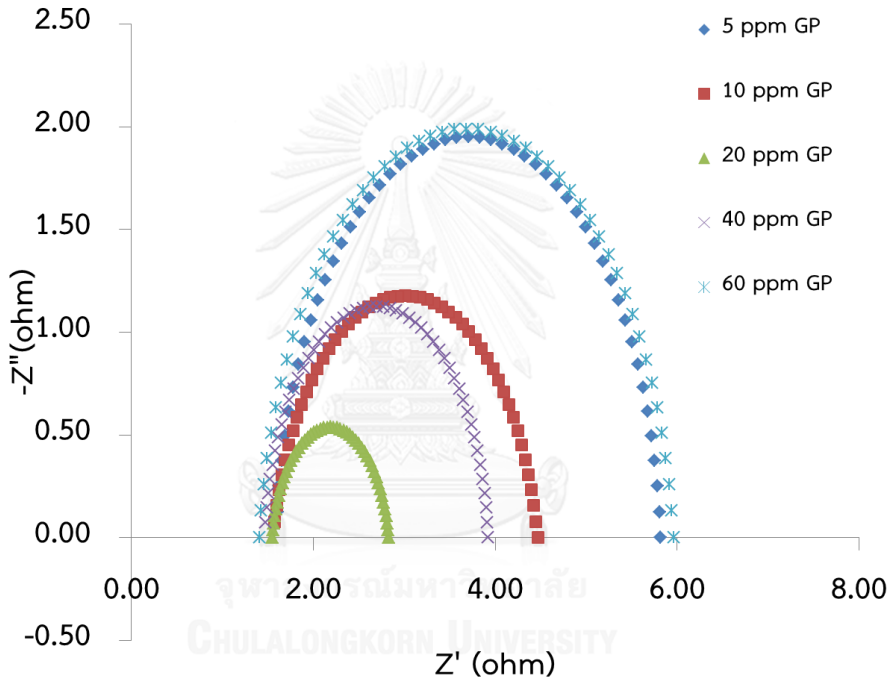

Figure 4.5 Nyquist plot of gelled electrolyte with different concentrations of GP at the frequency in the range of 10^{5} to 10^{-2} Hz at amplitude 10 mV.

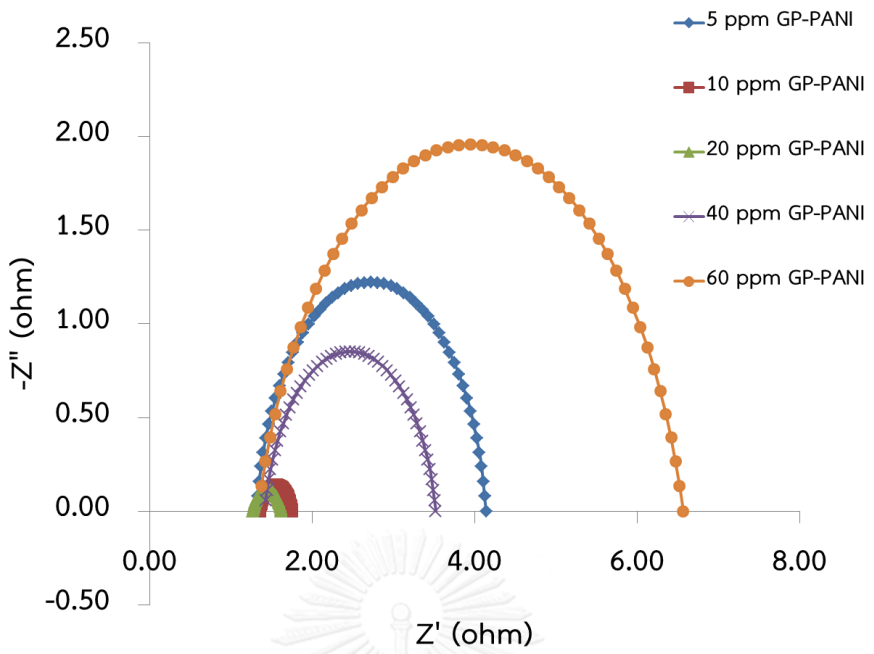

Figure 4.6 Nyquist plot of gelled electrolyte with different concentration of GP-PANI at the frequency in the range of 10^{5} to 10^{-2} Hz at amplitude 10 mV.

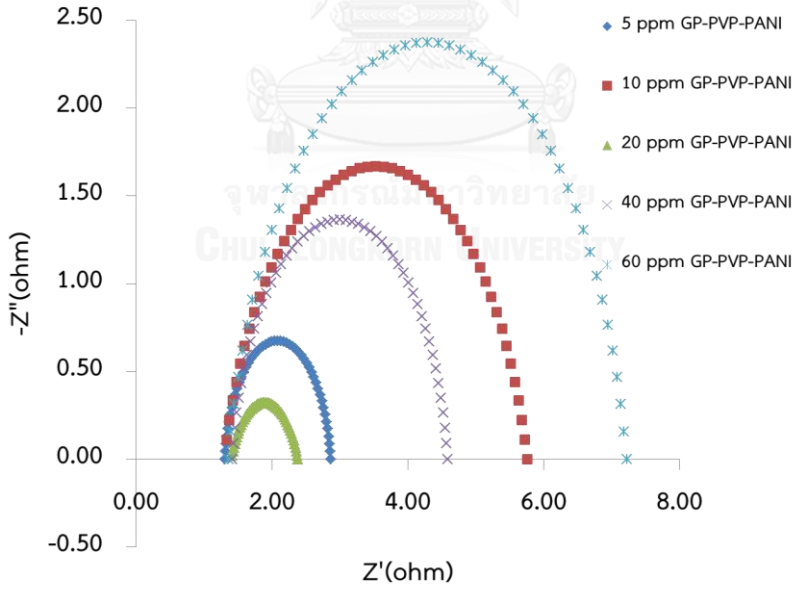

Figure 4.7 Nyquist plot of gelled electrolyte with different concentrations of GP-PVP- PANI at the frequency in the range of 10^{5} to 10^{-2} Hz at amplitude 10 mV.

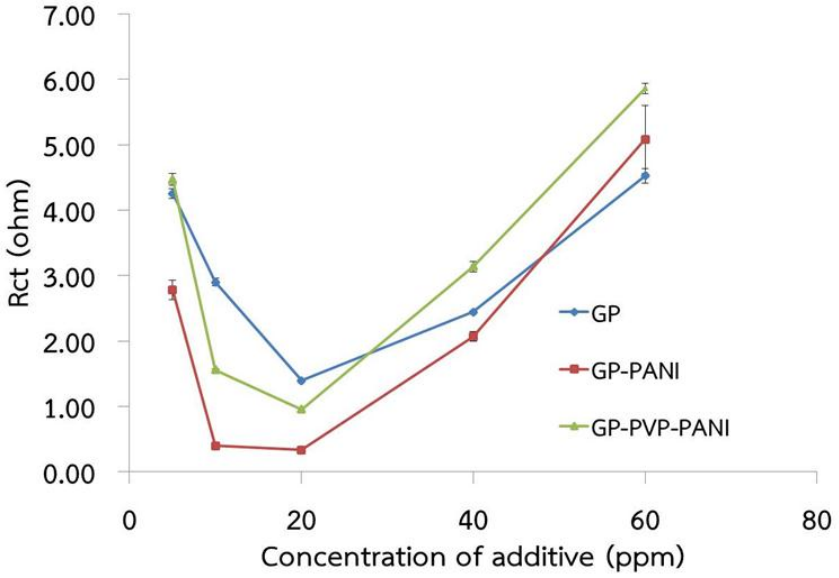

Figure 4.8 Charge transfer resistance (R_{ct}) of gelled electrolyte with different additives.

4.4 Battery Testing

4.4.1 Discharge Capacity

To study the cycling performance, GP, GP-PANI and GP-PVP-PANI were added to gelled electrolytes. The gelled electrolyte exhibiting the lowest charge transfer resistance was chosen to fill into the batteries in order to investigate the cycling performance. Figure 4.9 shows the discharge capacity during cycle life for gel batteries with various additives. The results show that gel batteries with GP-PANI perform the highest discharge capacity comparing to the other additives.

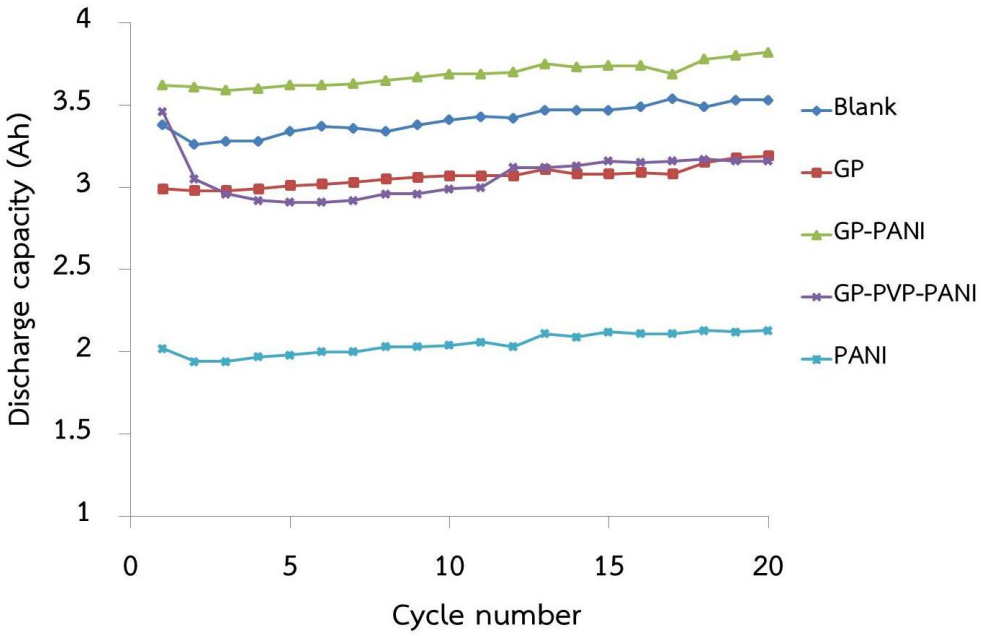

Figure 4.9 The discharge capacity of gel battery at different additive during 20 cycles.

To investigate long-term performance of battery with the different additives, the discharge capacity was measured under the 100% Depth of Discharge (DoD) at the high-rate discharge (1C) for 190 cycles at 25±2 °C. The discharge capacity of gel VRLA batteries prepared with 4% (w/v) SiO_2 and different additives were shown in Figure 4.10. The results show that the discharge capacity increased between 1 and 30 cycles while the discharge capacity decreased over 30 cycles. The AGM VRLA batteries filled with GP-PANI provided the highest discharge capacity. Comparing with the gel AGM VRLA battery in the absence of additive, the discharge capacity of gel AGM VRLA batteries was significantly improved by addition of GP-PANI. In contrast, addition of GP provided the decrease of discharge capacity compared to the absence of additive because GP showed high tendency to agglomerate and restack to form graphite through p–p stacking and Vander Waals interactions, which make the performance of gel AGM battery was decreased. Agglomeration can be reduced by the attachment of polymers to the graphene sheets. Moreover, the

addition of GP-PVP-PANI provided the decrease of discharge capacity compared to the presence of GP-PANI because PVP is a non-conducting polymer which may decrease conductivity of gelled battery. Thus, in this work, GP-PANI composite has been used as the additive for gel AGM VRLA battery. In summary, VRLA batteries containing with GP-PANI retain a discharge capacity above 3.25 Ah and have a discharge time longer than 27 min, which is higher than the JIS specification [46], even after 200 cycles at 100% DoD. The discharge capacity of the gelled electrolyte with 20 ppm GP-PANI is still slightly higher than that of the gelled electrolyte without additive.

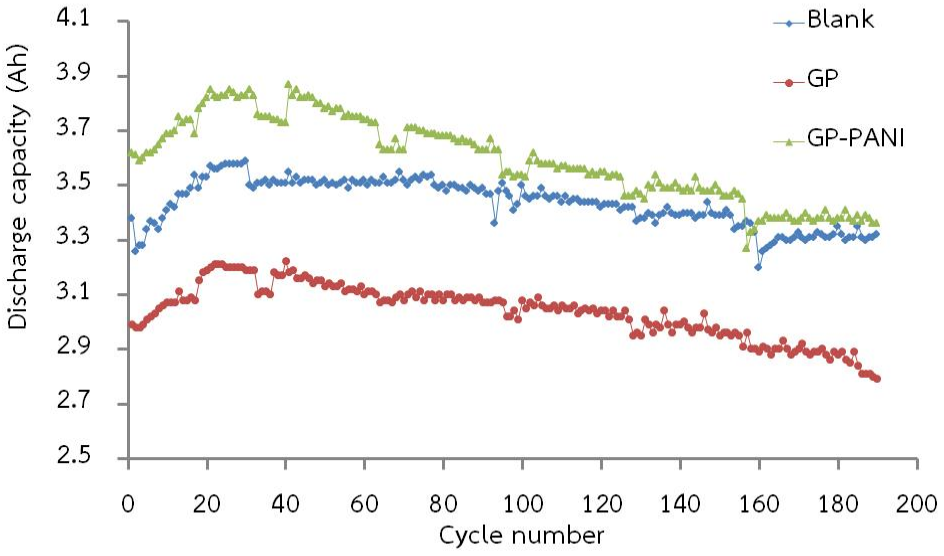

Figure 4.10 The discharge capacity of 4% (w/v) SiO_2 gel AGM VRLA batteries with various additives during 190 cycles.

4.4.2 Initial Discharge Curve of VRLA Batteries

Like the discharge capacity curve, initial discharge curve can be used to explain characteristics of battery. During discharging, the voltage will decrease until cut-off voltage (9.6V). The voltage characteristics of cell can be portrayed as a

plot of terminal voltage versus discharge time. Figure 4.11 shows the initial discharge curves of gelled electrolyte with various additives in gel AGM-VRLA batteries. Similarly to the discharge capacity results, gel battery containing GP-PANI showed the longest curves of the usage time in cycling. It means that tendency of discharge capacity is related to the initial discharge values. From both of criteria, it can be addressed that only GP-PANI can be used to improve performance of gel VRLA battery.

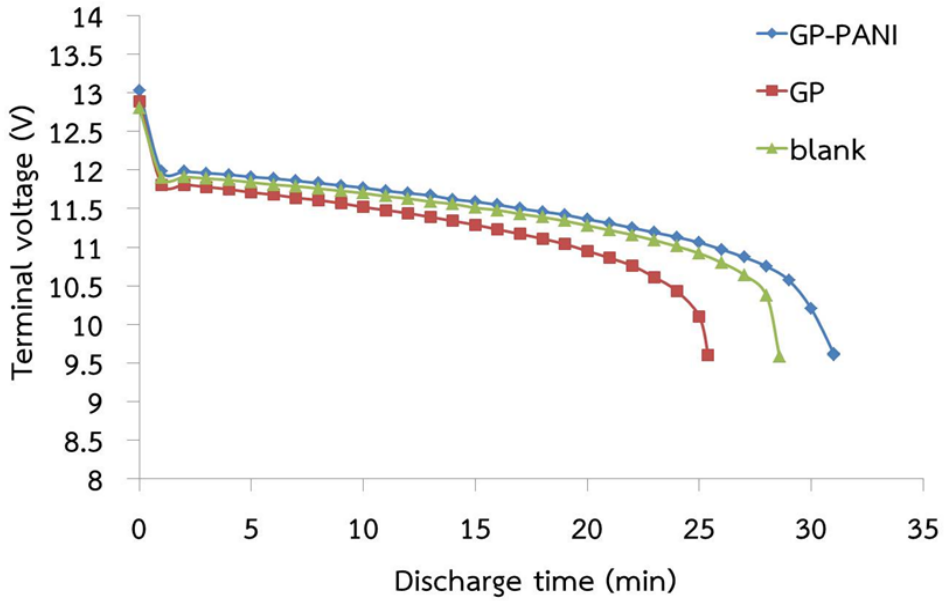

Figure 4.11 Initial discharge of various gel-batteries.

4.5 Characterization of Gelled electrolyte by FT-IR

The chemical structures of GP in fumed silica, GP-PANI composite in fumed silica and GP-PVP-PANI in fumed silica were depicted by FTIR spectra as shown in Figure 4.12, 4.13 and 4.14, respectively. The FT-IR spectrum of GP shows the broad peak at 3432 cm^{-1} corresponding to sp C-H stretching. The peaks observed at 2921 and 2840 cm^{-1} can be assigned to aromatic sp^2 C-H stretching. The peaks in the range of 1646 cm^{-1} attributed to in plane C=C bonds and the skeletal vibration of the

graphene sheets. The peaks at 1083 and 712 cm^{-1} correspond to sp^2 C-H bending [34, 47].

FT-IR spectrum of PANI shows the band observed at 3364 cm^{-1}, attributed to N-H stretching mode. The peaks located at 1579 cm^{-1} and 1478 cm^{-1} are ascribed to the C=C stretching deformation of quinoid ring benzenoid ring. The peak at 1309 cm^{-1} corresponds to the C-N stretching of secondary aromatic amines. The peaks at 1170 and 837 cm^{-1} can be attributed to aromatic C-H bending in-plane, out-of-plane for the 1,4-disubstitutedaromatic ring [47, 48].

The FTIR spectrum of fumed silica (SiO_2) shows the broad peak around 3412 cm^{-1} should be assigned to -OH- groups in water molecules. The peak at 1617 can be identified O–H bending vibration of adsorbed molecular water. The broad band at 1160 cm^{-1} corresponds to asymmetric stretching vibration of Si–O–Si bond. The peak observed at 804 cm^{-1} belong to Si–O bending vibration, and peak as shown at 448 cm^{-1} corresponds to Si–O rocking vibration [43, 49].

In addition, the spectrum of GP in fumed silica (SiO_2) appeared the characteristic peaks of both GP and SiO_2. The broad peak at 3432 cm^{-1} corresponds to C-H stretching of GP. For characteristic peak of SiO_2, the peak at 1131, 809 and 491 cm^{-1} are identical with peaks of stretching vibration of Si–O–Si bond, bending vibration and Si-O rocking vibration, respectively. The result indicates that GP exists in gelled electrolyte

For the GP-PANI composite in fumed silica (SiO_2), the FTIR spectra of this component were almost the same as the PANI spectra. The characteristic peaks of quinoid ring stretching at 1603 cm^{-1} and benzenoid ring stretching at 1338 cm^{-1} were observed. The peak at 864 is attributed to the out of plane bending of C-H. However, some peak which appeared at 3595 cm^{-1}, was originated from GP and the C-H bending peak shifts to a higher wave number (from 837 to 864 cm^{-1}) because of the π–π interaction and hydrogen bonding between the graphene sheets and PANI

in the composite [50]. This result indicates that the PANI are dropped on the graphene sheets successfully.

Finally, FTIR spectra of GP-PVP-PANI composite in fumed silica are almost the same as both PANI and GP spectra. The new peaks of PVP appear at approximately 1648-1654 cm^{-1}. This result indicates that GP-PVP-PANI exists in gelled electrolyte.

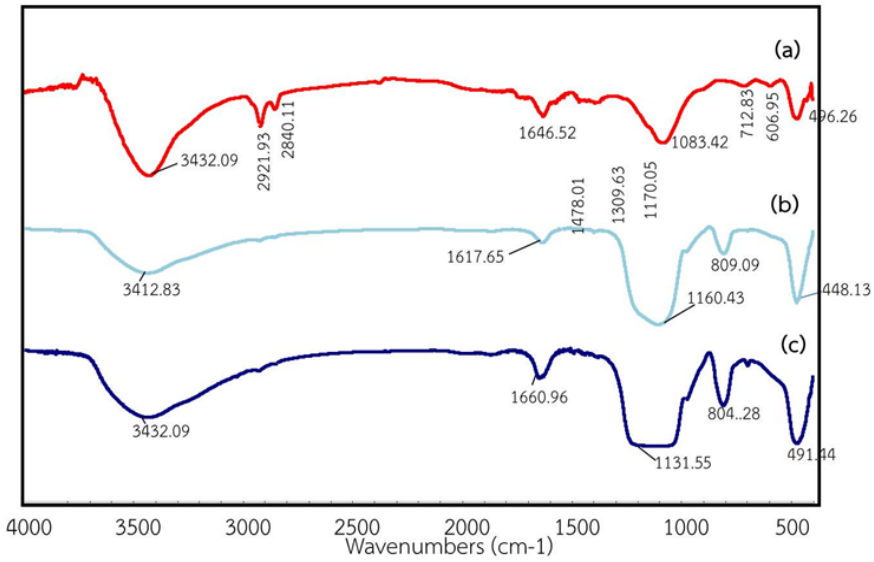

Figure 4.12 FT-IR spectra of (a) GP, (b) SiO_2 and (c) gelled electrolyte with GP (GP-SiO_2)

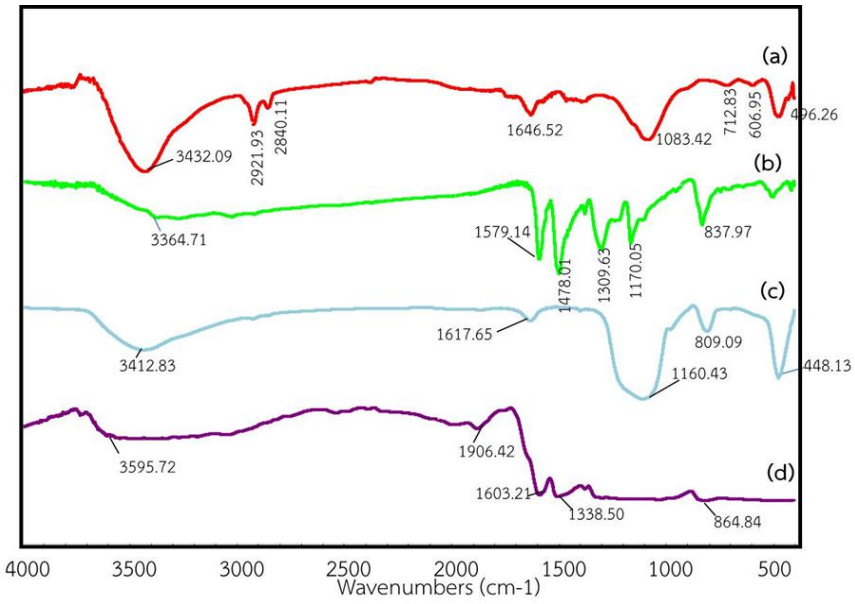

Figure 4.13 FT-IR spectra of (a) GP, (b) PANI, (C) SiO_2 and (d) gelled electrolyte with GP-PANI (GP-PANI-SiO_2)

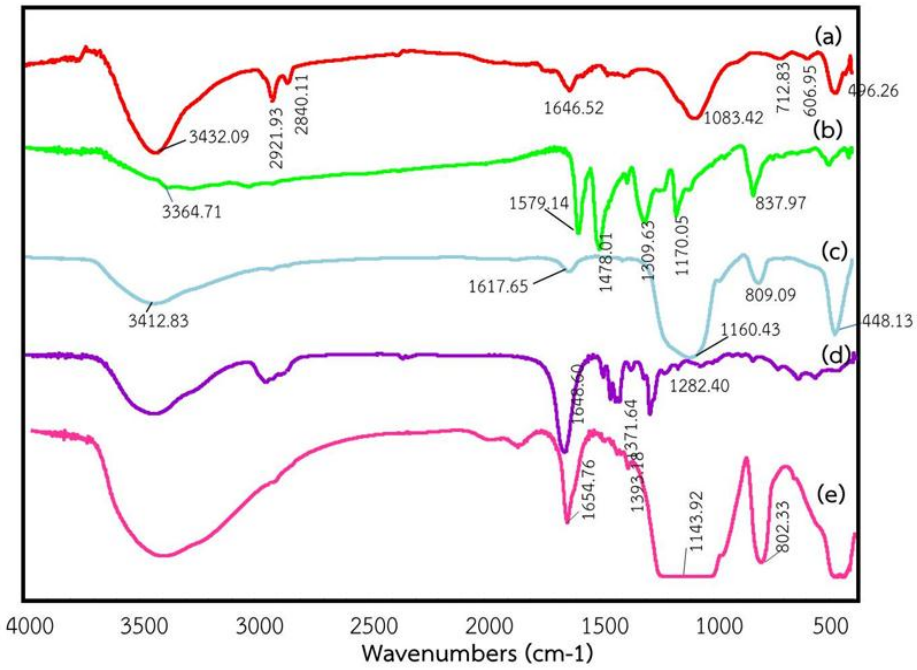

Figure 4.14 FT-IR spectra of (a) GP, (b) PANI, (C) SiO_2, (d) PVP and (e) gelled electrolyte with GP-PVP-PANI (GP-PVP-PANI-SiO_2)

4.6 Morphology of Gelled batteries

4.6.1 Morphology of Gelled electrolyte

After the battery test (section 4.4), the gel AGM VRLA batteries were cleaved and took the gelled electrolyte to investigate the morphology by scanning electron microscope (SEM). The morphology of gelled electrolytes from gel AGM VRLA batteries were shown in Figure 4.15. The large aggregations in fumed-silica gelled electrolyte may lead to poor contact between gel, plates and separators. The gelled electrolyte containing GP additive was dense and dryer than the other. Higher gel strength is good for leak avoidance but it is worse for electrolyte transference leading the discharging capacity decreases, hence the service life decreases. Interestingly, the morphology of gelled electrolyte containing GP-PANI showed

smooth surface. This morphology possibly caused the increasing of performance of battery.

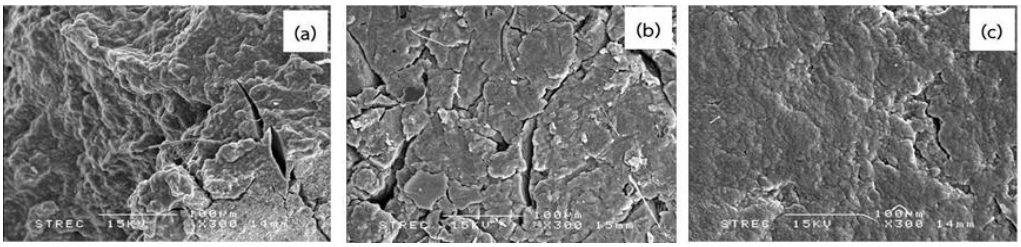

Figure 4.15 SEM images of gelled electrolyte from VRLA batteries after 190 cycle (a) absence additive (b) presence GP (c) presence GP-PANI

4.6.2 Morphology of Electrode

In order to study the effect of gelled electrolyte on the electrode morphology, the morphology of electrodes was investigated using scanning electron microscopy (SEM). Several factors may limit the capacity and cycle life of the lead acid batteries but one of the most important factors is related to the structural stability. It is important to keep the agglomerate skeleton at the cathode and to prevent the shrinkage of the anode. The agglomerate structure of the cathode collapsed after cycling. It resulted in the capacity loss of the battery.

In the presence of GP-PANI, the positive electrode remained the agglomerate skeleton better than the presence of only GP, the capacity loss is lower and the long cycle life is obtained.

The surface of the positive electrode for electrolyte containing GP was shown in Figure 4.16 (b). The small particles of $PbSO_4$ covered on electrode. That might increase the resistance of electrode and then resulted in the capacity loss in the battery. As a result, the GP in the gel battery probably caused the deformation of electrodes. The battery resistance was increased with the shrinkage of active material. It means that the ionic transfer had been disturbed, thus the

capacity was degraded. It was found that gel battery with GP provided lower discharge capacity than the one with GP-PANI.

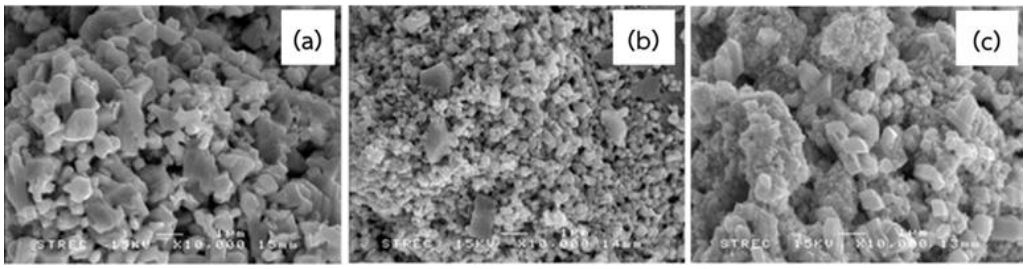

Figure 4.16 Morphology of PbO_2 electrode (Positive electrode) after charge-discharge 190 cycles (a) without additive, (b) with GP and (c) with GP-PANI

CHAPTER V

CONCLUSION

5.1 Conclusions

In conclusions, gelled electrolyte of valve-regulated lead-acid (VRLA) battery was prepared by mixing fumed silica, sulfuric acid solution, and additives. The concentration of fumed silica at 4% w/v was chosen because of suitable gelling time (more than 3 hr), and easy filling process. Moreover, the optimal concentration of the additive and type of additive was studied to improve gel characteristic and performance of battery. In this work, various additives added into gelled electrolyte were investigated, including graphene (GP), graphene-polyaniline (GP-PANI), and graphene-polyvinylpyrroridone-polyaniline (GP-PVP-PANI). The cyclic voltammetry was used to study water loss. Cyclic voltammograms ranging from -2.0 to 2.9 V at scan rate of 50 mV s^{-1} show the hydrogen and oxygen evolution. The gelled electrolyte containing GP-PANI showing the lowest hydrogen-oxygen evolution, corresponding to low water loss and long service life of battery, was achieved. To optimize concentration of additives, the electrochemical impedance spectroscopy (EIS) was used. The condition of EIS method was operated under the frequency in the range of 10^{5} to 10^{-2} Hz at amplitude of 10 mV. The gelled electrolyte containing GP-PANI showed the lowest charge transfer resistance comparing to the one containing only GP and GP-PVP-PANI. The gelled electrolyte containing 20 ppm GP-PANI provided the lowest charge transfer resistance corresponding to fast charge transfer. Moreover, the gelled electrolyte containing GP-PANI provided highest discharge, which is related to long service life. On the other hand, the gelled electrolyte containing GP provided the lowest discharge capacity and short service life. The morphology of electrode after the cycle life test was also studied. Using the gelled electrolyte containing GP-PANI, the positive electrode can keep the

agglomerate skeleton better than the one containing GP, and the capacity loss are lower than that leads to long cycle life.

The benefit of this work is that GP-PANI was firstly reported to use as the additive for the gel AGM VRLA batteries. The result obtained clearly displayed that the additive offers the significant improvement in performance of gelled electrolyte.

5.2 Future Perspective

According to an increase in performance in AGM VRLA batteries modified by GP-PANI composite, other GP-conducting polymers might improve battery performance. Therefore, other conducting polymers will be further investigated such as polypyrrole (PPy), Poly(3,4-ethylenedioxythiophene) (PEDOT) and Polystyrene sulfonate (PSS) which can be incorporated in the same way to improve the performance of VRLA batteries.

REFERENCES

[1] Martha, S.K., Hariprakash, B., Gaffoor, S.A., and Shukla, A.K. Performance characteristics of a gelled-electrolyte valve-regulated lead-acid battery. Bulletin of Materials Science 26(5) (2003): 465-469.

[2] Rezaei, B. and Taki, M. Effects of tetrabutylammonium hydrogen sulfate as an electrolyte additive on the electrochemical behavior of lead acid battery. Journal of Solid State Electrochemistry 12(12) (2008): 1663-1671.

[3] Rezaei, B., Mallakpour, S., and Taki, M. Application of ionic liquids as an electrolyte additive on the electrochemical behavior of lead acid battery. Journal of Power Sources 187(2) (2009): 605-612.

[4] Rezaei, B., Havakeshian, E., and Hajipour, A.R. Influence of acidic ionic liquids as an electrolyte additive on the electrochemical and corrosion behaviors of lead-acid battery. Journal of Solid State Electrochemistry 15(2) (2011): 421-430.

[5] Tantichanakul, T., Chailapakul, O., and Tantavichet, N. Influence of fumed silica and additives on the gel formation and performance of gel valve-regulated lead-acid batteries. Journal of Industrial and Engineering Chemistry 19(6) (2013): 2085-2091.

[6] Petkova, G., Nikolov, P., and Pavlov, D. Influence of polymer additive on the performance of lead-acid battery negative plates. Journal of Power Sources 158(2) (2006): 841-845.

[7] Tantichanakul, T., Chailapakul, O., and Tantavichet, N. Gelled electrolytes for use in absorptive glass mat valve-regulated lead-acid (AGM VRLA) batteries working under 100% depth of discharge conditions. Journal of Power Sources 196(20) (2011): 8764-8772.

[8] Valenciano, J., Sanchez, A., Trinidad, F., and Hollenkamp, A.F. Graphite and fiberglass additives for improving high-rate partial-state-of-charge cycle life of

valve-regulated lead-acid batteries. Journal of Power Sources 158(2) (2006): 851-863.

[9] Artiles, M.S., Rout, C.S., and Fisher, T.S. Graphene-based hybrid materials and devices for biosensing. Advanced Drug Delivery Reviews 63(14-15) (2011): 1352-1360.

[10] Wu, Q., Xu, Y.X., Yao, Z.Y., Liu, A.R., and Shi, G.Q. Supercapacitors Based on Flexible Graphene/Polyaniline Nanofiber Composite Films. Acs Nano 4(4) (2010): 1963-1970.

[11] Kim, T.Y., et al. High-Performance Supercapacitors Based on Poly(ionic liquid)-Modified Graphene Electrodes. Acs Nano 5(1) (2011): 436-442.

[12] Duraia, E.S.M., Mansurov, Z., and Tokmoldin, S. Formation of graphene by the thermal annealing of a graphite layer on silicon substrate in vacuum. Vacuum 86(2) (2011): 232-234.

[13] Novoselov, K.S., et al. Electric field effect in atomically thin carbon films. Science 306(5696) (2004): 666-669.

[14] Li, D., Muller, M.B., Gilje, S., Kaner, R.B., and Wallace, G.G. Processable aqueous dispersions of graphene nanosheets. Nature Nanotechnology 3(2) (2008): 101-105.

[15] Shan, C.S., Yang, H.F., Han, D.X., Zhang, Q.X., Ivaska, A., and Niu, L. Water-Soluble Graphene Covalently Functionalized by Biocompatible Poly-L-lysine. Langmuir 25(20) (2009): 12030-12033.

[16] Arya, S.K., Dey, A., and Bhansali, S. Polyaniline protected gold nanoparticles based mediator and label free electrochemical cortisol biosensor. Biosensors & Bioelectronics 28(1) (2011): 166-173.

[17] Tran, H.D., Li, D., and Kaner, R.B. One-Dimensional Conducting Polymer Nanostructures: Bulk Synthesis and Applications. Advanced Materials 21(14-15) (2009): 1487-1499.

[18] Li, D., Huang, J.X., and Kaner, R.B. Polyaniline Nanofibers: A Unique Polymer Nanostructure for Versatile Applications. Accounts of Chemical Research 42(1) (2009): 135-145.

[19] Kang, E.T., Neoh, K.G., and Tan, K.L. Polyaniline: A polymer with many interesting intrinsic redox states. Progress in Polymer Science 23(2) (1998): 277-324.

[20] Salkind, A.J., Hammel, R.O., Cannone, A.G., and Trumbore, F.A. Lead-acid battery. in, pp. 675-720: McGraw-Hill, 1994.

[21] The Encyclopedia of Alternative Energy and Sustainable Living. Lead-acid battery. [online] Available from: http://www.daviddarling.info/encyclopedia/L/AE_lead-acid_battery.html [2014, April 30]

[22] Mantell, C. Batteries and Energy Systems. second ed.: MacGraw-Hill, 1983.

[23] Berndt, D. Maintenance free batteries based on aqueous electrolyte lead-acid nickel/cadmium, nickel/hydride a handbook of battery technology. Great Britain: John Wiley and Sons, 2003.

[24] Oxide technology. Handbook for Stationary Lead-Acid Batteries. [online] 2012. Available from: http://www.exide.com/Media/files/Downloads/IndustEuro/Operating%20Instructions/Handbook,%20part%201,%20edition%206,%20Feb_%202012.pdf [2014, April 30]

[25] Culpin, B. and Rand, D.A.J. Failure modes of lead/acid batteries. Journal of Power Sources 36(4) (1991): 415-438.

[26] Lam, L.T., Haigh, N.P., Phyland, C.G., and Urban, A.J. Failure mode of valve-regulated lead-acid batteries under high-rate partial-state-of-charge operation. Journal of Power Sources 133(1) (2004): 126-134.

[27] Nakamura, K., Shiomi, M., Takahashi, K., and Tsubota, M. Failure modes of valve-regulated lead/acid batteries. Journal of Power Sources 59(1-2) (1996): 153-157.

[28] Wagner, R. Failure modes of valve-regulated lead-acid-batteries in different applications. Journal of Power Sources 53(1) (1995): 153-162.

[29] MIT Electric Vehicle Team. A Guide to Understanding Battery Specifications. [online] 2008. Available from: http://web.mit.edu/evt/summary_battery_specifications.pdf [2014, April 30]

[30] Rush, W., Vassallo, K., and Heart, G. Undersranding the real differencees between gel and AGM batteries. [online] 2007. Available from: http://www.battcon.com/paperfinal2007/rushpaper2007.pdf [2014, April 30]

[31] Raghavan, S.R., Walls, H.J., and Khan, S.A. Lithium/V_3O_{13} cells using silica nanoparticle-based composite electrolyte. Langmuir 16 (2000): 7920-7930.

[32] Wajid, A.S., et al. Polymer-stabilized graphene dispersions at high concentrations in organic solvents for composite production. Carbon 50(2) (2012): 526-534.

[33] Ruecha, N., Rangkupan, R., Rodthongkum, N., and Chailapakul, O. Novel paper-based cholesterol biosensor using graphene/polyvinylpyrrolidone/polyaniline nanocomposite. Biosensors and Bioelectronics 52(0) (2014): 13-19.

[34] Zheng, Z.X., Du, Y.L., Feng, Q.L., Wang, Z.H., and Wang, C.M. Facile method to prepare Pd/graphene-polyaniline nanocomposite and used as new electrode material for electrochemical sensing. Journal of Molecular Catalysis a-Chemical 353 (2012): 80-86.

[35] Bard, A.J. and Faulkner, L.R. Fundamentals and Applications. 2nd ed. New York, USA: Jonh Wiley & Sons, 2001.

[36] Skoog, D.A., Holler, F.J., and Nieman, T.A. Principles of Instrumental Analysis. New York, USA: Harcourt Brace College, 1998.

[37] Orazem, M.E. and Bernard, T. Electrochemical Impedance Spectroscopy. John Wiley & Sons,, 2008.

[38] Dietz, H., Hoogestraat, G., Laibach, S., von Borstel, D., and Wiesener, K. Influence of substituted benzaldehydes and their derivatives as inhibitors for hydrogen evolution in lead/acid batteries. Journal of Power Sources 53(2) (1995): 359-365.

[39] Karimi, M.A., Karami, H., and Mahdipour, M. Sodium sulfate as an efficient additive of negative paste for lead-acid batteries. Journal of Power Sources 160(2) (2006): 1414-1419.

[40] Chaiyasit, A. Effect of polymers on gel electrolyte properties in lead-acid battery. Master's Thesis, Faculty of science, Petrochemistry and polymer science, Chulalongkorn university, 2008.

[41] Siridetpan, W. Development of gelled electrolyte for lead acid battery using polyacrylamide and sulfate salts. Master's Thesis, Faculty of Science, Petrochemistry and polymer science, Chulalongkorn university, 2008.

[42] Pavlov, D., Rogachev, T., Nikolov, P., and Petkova, G. Mechanism of action of electrochemically active carbons on the processes that take place at the negative plates of lead-acid batteries. Journal of Power Sources 191(1) (2009): 58-75.

[43] Pan, K., et al. The performance of a silica-based mixed gel electrolyte in lead acid batteries. Journal of Power Sources 209 (2012): 262-268.

[44] Berndt, D. Mainternance-free Batteries Lead acid ,Nickel/cadmium,Nickel/hydride a Handbook of Battery Technology. Great Briain, 1993.

[45] Vinod, M.P. and Vijayamohanan, K. Effect of gelling on the impedance parameters of Pb/PbSO4 electrode in maintenance-free lead-acid batteries. Journal of Power Sources 89(1) (2000): 88-92.

[46] Japanese Indrustial Standard. Small-size valve regulated lead-acid batteries Plate 1: General requirements, functional characteristics method of test. JIS C 8702-1 (2003): 4-8.

[47] Yan, X.B., Han, Z.J., Yang, Y., and Tay, B.K. NO_2 gas sensing with polyaniline nanofibers synthesized by a facile aqueous/organic interfacial polymerization. Sensors and Actuators B: Chemical 123(1) (2007): 107-113.

[48] Cruz-Silva, R., et al. Comparative study of polyaniline cast films prepared from enzymatically and chemically synthesized polyaniline. Polymer 45(14) (2004): 4711-4717.

[49] Tang, Z., et al. Investigation and application of polysiloxane-based gel electrolyte in valve-regulated lead-acid battery. Journal of Power Sources 168(1) (2007): 49-57.

[50] Liu, H., Wang, Y., Gou, X., Qi, T., Yang, J., and Ding, Y. Three-dimensional graphene/polyaniline composite material for high-performance supercapacitor applications. Materials Science and Engineering: B 178(5) (2013): 293-298.

APPENDIX

APPENDIX A

Figure A1 Characteristic of gelled electrolyte in AGM VRLA battery

APPENDIX B

Table B1 The discharge capacity of gel AGM VRLA batteries at different additive during 20 cycles

Cycle number	Discharge capacity (Ah)				
	Blank	GP	PANI	GP-PANI	GP-PVP-PANI
1	3.38	2.99	2.02	3.62	3.46
2	3.26	2.98	1.94	3.61	3.05
3	3.28	2.98	1.94	3.59	2.96
4	3.28	2.99	1.97	3.60	2.92
5	3.34	3.01	1.98	3.62	2.91
6	3.37	3.02	2.00	3.62	2.91
7	3.36	3.03	2.00	3.63	2.92
8	3.34	3.05	2.03	3.65	2.96
9	3.38	3.06	2.03	3.67	2.96
10	3.41	3.07	2.04	3.69	2.99
11	3.43	3.07	2.06	3.69	3.00
12	3.42	3.07	2.03	3.70	3.12
13	3.47	3.11	2.11	3.75	3.12
14	3.47	3.08	2.09	3.73	3.13
15	3.47	3.08	2.12	3.74	3.16
16	3.49	3.09	2.11	3.74	3.15
17	3.54	3.08	2.11	3.69	3.16
18	3.49	3.15	2.13	3.78	3.17
19	3.53	3.18	2.12	3.80	3.16
20	3.53	3.19	2.13	3.82	3.16

APPENDIX C

Table C1 The discharge capacity of gel AGM VRLA batteries at different additive during 190 cycles.

Cycle number	Discharge capacity (Ah)		
	Blank	GP	GP-PANI
1	3.38	2.99	3.62
2	3.26	2.98	3.61
3	3.28	2.98	3.59
4	3.28	2.99	3.60
5	3.34	3.01	3.62
6	3.37	3.02	3.62
7	3.36	3.03	3.63
8	3.34	3.05	3.65
9	3.38	3.06	3.67
10	3.41	3.07	3.69
11	3.43	3.07	3.69
12	3.42	3.07	3.70
13	3.47	3.11	3.75
14	3.47	3.08	3.73
15	3.47	3.08	3.74
16	3.49	3.09	3.74
17	3.54	3.08	3.69
18	3.49	3.15	3.78
19	3.53	3.18	3.80
20	3.53	3.19	3.82
21	3.57	3.20	3.85
22	3.56	3.21	3.83
23	3.56	3.21	3.82
24	3.57	3.21	3.83
25	3.58	3.20	3.83

Cycle number	Discharge capacity (Ah)		
	Blank	GP	GP-PANI
26	3.58	3.20	3.85
27	3.58	3.20	3.84
28	3.58	3.20	3.82
29	3.58	3.20	3.83
30	3.59	3.19	3.83
31	3.50	3.19	3.85
32	3.49	3.19	3.83
33	3.51	3.10	3.76
34	3.51	3.11	3.75
35	3.52	3.11	3.75
36	3.50	3.10	3.75
37	3.52	3.18	3.74
38	3.51	3.17	3.74
39	3.51	3.17	3.73
40	3.51	3.22	3.73
41	3.55	3.18	3.87
42	3.51	3.19	3.83
43	3.53	3.16	3.85
44	3.51	3.16	3.82
45	3.52	3.17	3.82
46	3.52	3.16	3.83
47	3.52	3.14	3.82
48	3.50	3.15	3.80
49	3.51	3.15	3.80
50	3.52	3.13	3.78
51	3.50	3.14	3.79
52	3.51	3.13	3.77

Cycle number	Discharge capacity (Ah)		
	Blank	GP	GP-PANI
53	3.50	3.13	3.78
54	3.51	3.14	3.78
55	3.52	3.11	3.75
56	3.49	3.12	3.76
57	3.52	3.12	3.75
58	3.51	3.11	3.75
59	3.51	3.13	3.75
60	3.52	3.10	3.74
61	3.50	3.11	3.74
62	3.52	3.11	3.73
63	3.51	3.10	3.73
64	3.51	3.07	3.65
65	3.53	3.08	3.63
66	3.51	3.08	3.63
67	3.51	3.07	3.63
68	3.52	3.09	3.67
69	3.55	3.10	3.63
70	3.52	3.08	3.63
71	3.50	3.10	3.71
72	3.52	3.11	3.71
73	3.53	3.09	3.71
74	3.52	3.11	3.70
75	3.54	3.08	3.70
76	3.53	3.10	3.69
77	3.54	3.10	3.69
78	3.50	3.08	3.69

Cycle number	Discharge capacity (Ah)		
	Blank	GP	GP-PANI
79	3.49	3.10	3.68
80	3.50	3.08	3.68
81	3.48	3.10	3.68
82	3.50	3.10	3.68
83	3.50	3.08	3.67
84	3.49	3.09	3.66
85	3.49	3.08	3.67
86	3.48	3.09	3.66
87	3.50	3.09	3.66
88	3.49	3.08	3.65
89	3.48	3.09	3.63
90	3.49	3.07	3.63
91	3.47	3.07	3.63
92	3.47	3.07	3.67
93	3.36	3.08	3.63
94	3.48	3.08	3.63
95	3.51	3.07	3.54
96	3.48	3.02	3.55
97	3.46	3.02	3.55
98	3.41	3.04	3.53
99	3.43	3.01	3.54
100	3.50	3.08	3.54
101	3.46	3.05	3.53
102	3.45	3.07	3.59
103	3.46	3.06	3.62
104	3.46	3.09	3.59
105	3.49	3.06	3.58

Cycle number	Discharge capacity (Ah)		
	Blank	GP	GP-PANI
106	3.46	3.05	3.58
107	3.45	3.05	3.58
108	3.46	3.06	3.58
109	3.46	3.04	3.56
110	3.44	3.06	3.57
111	3.46	3.05	3.57
112	3.44	3.05	3.56
113	3.45	3.06	3.56
114	3.45	3.03	3.56
115	3.44	3.04	3.56
116	3.44	3.05	3.56
117	3.44	3.04	3.54
118	3.44	3.05	3.55
119	3.44	3.03	3.54
120	3.42	3.04	3.55
121	3.43	3.04	3.55
122	3.43	3.02	3.53
123	3.43	3.04	3.54
124	3.43	3.02	3.54
125	3.41	3.02	3.53
126	3.42	3.04	3.46
127	3.42	3.01	3.46
128	3.42	2.95	3.46
129	3.37	2.96	3.48
130	3.38	2.95	3.47
131	3.38	3.01	3.45
132	3.40	2.99	3.50

Cycle number	Discharge capacity (Ah)		
	Blank	GP	GP-PANI
133	3.39	2.96	3.49
134	3.36	2.99	3.54
135	3.39	2.98	3.51
136	3.40	3.04	3.49
137	3.42	2.99	3.49
138	3.40	2.96	3.49
139	3.39	2.99	3.51
140	3.39	2.99	3.49
141	3.40	3.00	3.48
142	3.40	2.98	3.49
143	3.40	2.96	3.48
144	3.38	2.98	3.53
145	3.39	2.98	3.49
146	3.39	3.03	3.48
147	3.44	2.97	3.48
148	3.40	2.96	3.48
149	3.39	2.98	3.50
150	3.39	2.95	3.48
151	3.39	2.96	3.46
152	3.41	2.96	3.46
153	3.39	2.95	3.46
154	3.34	2.96	3.48
155	3.35	2.95	3.47
156	3.35	2.91	3.45
157	3.37	2.96	3.27
158	3.36	2.90	3.33
159	3.33	2.90	3.34

Cycle number	Discharge capacity (Ah)		
	Blank	GP	GP-PANI
160	3.20	2.89	3.37
161	3.26	2.91	3.37
162	3.27	2.90	3.39
163	3.28	2.88	3.38
164	3.29	2.90	3.38
165	3.31	2.90	3.38
166	3.31	2.93	3.38
167	3.30	2.90	3.40
168	3.30	2.88	3.38
169	3.31	2.89	3.37
170	3.33	2.90	3.37
171	3.31	2.92	3.38
172	3.30	2.89	3.40
173	3.31	2.88	3.38
174	3.31	2.89	3.37
175	3.33	2.89	3.38
176	3.32	2.90	3.38
177	3.31	2.88	3.41
178	3.31	2.86	3.38
179	3.32	2.89	3.37
180	3.35	2.88	3.38
181	3.32	2.89	3.38
182	3.30	2.86	3.41
183	3.31	2.85	3.38
184	3.31	2.89	3.37
185	3.35	2.84	3.39
186	3.31	2.81	3.37

Cycle number	Discharge capacity (Ah)		
	Blank	GP	GP-PANI
187	3.30	2.81	3.39
188	3.31	2.81	3.38
189	3.31	2.80	3.36
190	3.32	2.79	3.36

VITA

Miss Suladda Prachanklang was born on November, 1st 1986 in Nakhonratchasima, Thailand. She graduated with high school degree from Phoowittaya School, Nakhonratchasima in 2005. She received her Bachelor's degree of Science (Chemistry) from Srinakharinwirot University in 2009. After that, in 2011, she has become a graduate student in the Petrochemistry and Polymer Science, Faculty of Science, Chulalongkorn University. In addition, she was a member of Electrochemical and Optical Spectroscopy Research Unit (EOSRU) under the direction of Professor Dr. Orawon Chailapakul. She graduated with Master's degree in chemistry of academic year 2014 from Chulalongkorn University.

Publication

Prachanklang, S., Siangproh, W., and Chailapakul, O. (January 8-10,2014) lnfuence of graphene-polyaniline additive on the performance of gel valve regulated lead-acid battery. Proceeding of Pure and Applied Chemistry International Conference 2014 (PACCON2014), Khon Kaen,Thailand.